NTNU

Norwegian University of
Science and Technology

An Integrated Tool for Microgrid Design in Rural Areas

Håkon Duus

Master of Energy and Environmental Engineering
Submission date: November 2015
Supervisor: Olav B Fosso, ELKRAFT
Co-supervisor: Marta Molinas, ITK

Norwegian University of Science and Technology
Department of Electric Power Engineering

ABSTRACT

PV-microgrids are becoming an affordable alternative to provide electricity access to remote or isolated regions, due to both a reduction in prices on solar panels and a strong focus on utilisation renewable energy resources.

When designing microgrids, the use of optimization methods has traditionally been rather limited. Flexible systematic design tools that covers the full system path from data-acquisition to optimization and load-flow-analysis, are of limited availability.

This thesis will seek to present a methodology for a cost-effective design of microgrids based on composable tools using optimization. Possible ways to overcome the lack of data will be discussed, along with the economic parameters used for the optimization process. A selection of already-existing tools will be presented, along with the advantages of the using novel sizing methodology presented in the thesis.

The methodology presented will be applied to a case-study in Bhutan. Using measured data from the study, the accuracy of initial assumptions and data-acquisition can be evaluated. The findings were that initial assumptions can give a good idea on consumer behaviour, and thus system composition, however a more detailed study on local conditions will always be preferred.

Finally stable operation of the optimized system will be validated through Matlab/Simulink-models.

SAMMENDRAG

PV-mikrogrids blir et stadig mer prisgunstig alternativ for kraftproduksjon i grisgrente strøk, både grunnet det kraftige fallet i pris på solceller, i tillegg til et økt fokus på bruk av fornybar energi.

Bruken av optimaliseringverktøy i designprosessen til mikrogrids har tradisjonelt vært heller begrenset. Det finnes få fleksible verktøy som dekker hele prosessen fra datainnsamling, til optimalisering og lastflytanalyse.

Denne oppgaven har som formål å presentere en metodologi for kostnadseffektive design-løsninger for mikrogrids, basert på sammen-settbare optimaliseringsverktøy. Ulike måter å takle manglende data på, samt de øknomiske parameterne som danner grunnlaget for optimaliseringen, vil bli diskutert. Et utvalg av slike verktøy som allerede er på markedet kommer til å bli presentert, sammen med fordelene til den nye metodologien.

Dette nye verktøyet vil bli anvendt på en case-studie i Bhutan. Ved bruk av målte data fra denne studien, kan treffsikkerheten til de opprinnelige antagelsene og dataene bli evaluert. Resultatene var at disse opprinnelige antagelsene gave en god pekepinn på forbruksmønster, og således systemsammensetning, men mer detaljert informasjon om lokale forhold er stadig å foretrekke.

Avslutningsvis vil det bli brukt Matlab/Simulink-modeller for å bekrefte at det optimaliserte systemet opererer stabilt.

You westerners are too concerned with time

— Karma Sampo

ACKNOWLEDGMENTS

First of all i would like to thank Marta Molinas for giving me the great opportunity to partake in this project, for insightful and rewarding discussions, and valuable feedback throughout the process. Olav Fosso for helpful supervision and guidance on technical writing.

My co-worker and travel-partner Geir Kulia for patience and support both on the technical part, as well as during the field-trip to Bhutan.

The summer-internship-team at NTNU with especial emphasis on Anne Lozé, Danielle Sakepa, Jeemijn Scheen and Honorad Quinard for great discussion and cooperation.

And last, but not at all least, the students and staff at the College of Science and Technology in Phuentsholing, Bhutan, for making it all a life-changing experience.

My most sincere thanks to you all.

CONTENTS

LIST OF FIGURES

LIST OF TABLES

1 INTRODUCTION

1.1 MOTIVATION FOR THE TOPIC

With the awareness of climate change and increased focus on renewable energies, the need for proper methods of optimizing the energy-systems of tomorrow are needed. According to the International Energy Agency (IEA) [21], over 1.3 billion people lack access to electricity, the vast majority (95%) being in Sub-Saharan Africa or developing countries in Asia. Also, 85% of these 1.3 billions are in rural areas. To make the largest impact, the focus for providing electricity should then be in rural areas, in these parts of the world. Providing sustainable and affordable energy for the entire worlds population is also one of the Unites Nations Sustainability Goals [51].

Utilizing microgrids to provide electricity is becoming increasingly popular, and several initiatives working to promote such solutions exist worldwide. A microgrid is a small electric power system with a production-unit, some form of storage and a load. Production-units could be PV, wind-power or a diesel aggregate, or a combination of these. It is further implied that microgrids are islanded grids, which operates autonomously.

Currently diesel aggregates are often used for electricity production in rural areas, but with the continued drop in prices on solar panels, these are quickly becoming a viable option to conventional fossile fuels according to University of New South Wales, Australia [52].

Further motivation for the topic is found in the book "Small is Beautiful" by Schumacher [43]. He argues that we must change the destructive trends we now see in technology, and the over-exploitation of natural resources, such as fossile fuels. He sums it up like this:

> What is it that we really require from the scientists and technologists? I should answer: We need methods and equipments which are
>
> – cheap enough so that they are accessible to virtually everyone;
>
> – suitable for small-scale application; and
>
> – compatible with man's need for creativity.

These are the key-elements of this thesis. An open-source software for dimensioning and assessing microgrids, with a bottom-up approach especially targeted for small-scale applications in rural areas.

1.2 THESIS SCOPE

The purpose of this thesis is to make a first step towards an open-source flexible tool for dimensioning microgrids in developing countries.

When designing microgrids, the use of optimization methods covering the full path, from resource assessment, to finished and operating system with load-flow-analysis has traditionally been rather limited. Flexible systematic design tools that can adapt to different project sizes, the lack of data, and the different systems constraints, are of limited availability.

There are, however, numerous programs and tools for evaluating different steps of the process. As many as 37 such tools was revised in Connolly et al. [9], with the purpose of giving the reader an overview of the options, and some guidance in which tool that would be best suited for the purpose. Another paper, Bhattacharyya [5], explores the different methodologies typically utilized by such optimization tools, and presents five methodological approaches for system optimization. It points out the lack of programs covering the full system-path, from resource assessment to an operating system model, and also the lack tools designed specifically for developing countries.

This thesis will seek to present a methodology for a cost-effective design of microgrids in rural areas, based on composable tools using optimization. Possible ways to overcome the lack of data will be discussed, and different tools to optimize the system in the best possible way for the consumer, within given constraints will be presented. Stable operation of the complete system will be validated utilizing MATLAB / Simulink models.

Furthermore, the program will be open-source and free to use, and expensive licences are not adding to the system expenditure. With an open source program, the basic assumptions can be checked, tweaked and changed by the final user, if necessary. This is not possible with many of the already-existing commercial softwares, which are closed-source programs. Here it is also difficult to understand the basic assumptions made by throughout the optimization and simulation process.

The foundation for such a flexible tool is found in Mandelli [28], and it will be used in this thesis as a basis for continued development towards a complete tool, addressing the full process of planning and optimizing a microgrid. Tools for investigating annual and daily performance will be added to this base. This program, as well as the methodology used will henceforth be referred to as "the novel sizing methodology".

To validate the reliability and usefulness of said methodology, it will be applied to a case study at the College of Science and Technology (CST), in Phuentsholing, Bhutan. During the course of the thesis, a four week long field-trip was done to the CST to get a better understanding of the local conditions, in addition to investigating if the preliminary assumptions made in Norway, would in fact resemble the real case in Bhutan. More details on the case study and field-trip is found in Section 2.1 and in Appendix B.

1.3 RELATION TO SPECIALIZATION PROJECT

During the fall in 2014, a preliminary study of the novel sizing methodology was conducted. The cooperation with CST in regards to this project was initiated, and some basic assumptions on electric consumption and local conditions in Bhutan were made based on correspondence with students and staff.

The work resulted in the paper Duus et al. [13], and some of this information is recited in this thesis. It also describes in more detail the motivation of the project from CSTs' side, the larger drivers being energy security in Bhutan with increased power production from multiple sources, combined with building knowledge capacity at the university.

1.4 THESIS OUTLINE

The thesis will first describe the collection of data, what data is necessary, and how it can be accessed or synthesized. The validity of this data will also be discussed, and how this will impact the system as a whole.

It will then go on to describe the economics of the system, and how this parameter in many ways is decisive for system optimization and design.

When all necessary data and parameters required for the optimization process are outlined, a small selection of already-existing optimization tools will be presented, along with the novel sizing methodology. Having both synthesized data and measured data from Bhutan present, several optimal systems will be made in order to evaluate whether the initial assumptions will result in a system resembling the real case. The systems will further be evaluated on performance through yearly and daily simulations by using Matlab and Simulink.

Measured data from Bhutan will be compared with the collected data presented throughout the earlier chapters, and comments will be made explaining deviations and possible improvements to be done in data-collection and base assumptions for further systems.

2 RESOURCE ASSESSMENT

When designing a microgrid, or any kind of grid, the data used to design and size the system is imperative for the outcome.

In rural areas, the amount of data can be limited, which poses challenges to the accuracy of the design and optimization of the grid. This chapter will cover the most basic aspects of the data-acquisition, namely the resource assessment. It will seek to overcome some of these challenges by using freely available satellite data, and further present a methodology to estimate the load of the system.

2.1 EXPLANATION AND DESCRIPTION OF THE CASE STUDY

In order to properly test the methodology presented in the thesis, it is to be applied to a real case. For this reason, from September 18th to October 20th, the author of the thesis, together with Mr. Geir Kulia, travelled to Bhutan and conducted a field-study at the College of Science and Technology (CST) in Phuentsholing. The goal was to better understand the local conditions, and what particular considerations which should be made. Here follows some of the observations and experiences from the stay.

At the present time (fall 2015), there are about 860 students living at the CST campus, divided in 7 hostel-blocks; Block-A, Block-B, Block-C, Block-D, Block-E, RK Hostel LH, RK Hostel RH.

Block-A to Block-D are equal, with 3 floors, and 13 rooms on the ground floor and 14 rooms on 2nd and 3rd floor, totalling 41 rooms.

Hostel LH and RH are also the same, each with 4 floors, and 12 rooms per floor, giving a total of 48 rooms per hostel.

Block-E has two floors, with 12 and 33 rooms respectfully. The school canteen is also situated on the ground floor of Block-E.

Adding up all the rooms at campus gives a total of 305 rooms, accommodating all of the students. An areal view of the campus is given in Figure 2.1.

There are at least two students living in each room, but the most common is three living together in one room. All of the rooms are equipped with more or less the same electrical appliances, such as lights, fans, and charging for cellphones and laptops. Each floor has shared bathroom-facilities.

Electricity is used mainly for lightning and fans, as it is relatively warm during daytime, and even at night during summer and monsoon. Night-temperatures of $25 - 30°C$ are normal in this season.

A typical school-day is class from 8-12, lunch is served at 12, and then typically laboratory work or more classes from 13 - 16. After class the students either study or participate in leisure-activities, such as football. These activities usually end at sunset, which is at about 18h in September-October.

After sunset, most students go to their rooms, hang out, and are social. This is also very visible on electric consumption, as they now use fans and lights in their rooms much more than during daytime.

All meals are made in the canteen, including dinner, which is served at 19. Not much cooking is done in the hostel by the students individually.

2.2 ACQUIRING SOLAR IRRADIANCE DATA

Output power generated from the solar panels depends on the solar irradiance, and the panel temperature. To have any idea on the output power, these two parameters must be found for the area in question. It can be acquired either through satellite measurements, or by installing ground-measurement-equipment on-site. The latter is a much more expensive alternative, as satellite data is found freely available online. One would also assume that ground-measurements always would be more accurate, but if the site in question is not very closely situated to the ground-measurement apparatus, satellite-data might be more accurate. This will be discussed in more detail in Section 2.2.3.

2.2.1 *Note on terminology*

Several different terminologies are used to explain the energy and power given from the sun to the earth, but with somewhat different meaning and unit.

In the following, a clarification on how the terminology is used in this thesis will be presented, in an attempt to avoid confusion.

2.2.1.1 *Irradiance*

Irradiance is the amount of solar energy delivered to a surface area A at a given time, giving it the unit W/m^2. It is a measurement of power per surface area, and thus is dimensioning for the power possible to extract from the PV-panels.

The equation is shown below:

$$E = W/m^2 \tag{2.1}$$

Figure 2.1: Model showing the campus of CST. The long yellow building to the mid-left is Block-E with the canteen. The two squared buildings with red roof are Block-A to Block-D, and the two orthogonal buildings just opposed to Block-A are Hostel RK and LH.

Irradiation on the other hand describes the process of being exposed to radiance, and is thus not a physical measure. It will not be used in this thesis.

2.2.1.2 *Insolation*

Insolation is the total amount of energy that has been collected on a surface area within a given time period. While the irradiance denotes the instantaneous rate in which power is delivered to a surface, insolation denotes the cumulative sum of all the energy striking the surface area for a given time interval, typically one hour. In other words it is the time-integral of irradiance, giving the unit:

$$\mathrm{Insolation} = Wh/m^2 \tag{2.2}$$

Having an average hourly measurement of irradiance of an area, would thus result in irradiance and insolation being "equal" in sense of value, but not in the sense of unit.

For all uses and purposes, irradiance data will be used in the paper, unless otherwise specified.

2.2.1.3 *GHI, DNI og DHI*

The total solar irradiance (TSI) that hits the earth, can be broken down into three main components; Direct Normal Irradiance (DNI), Direct Horizontal Irradiance (DHI) and Global Horizontal Irradiance (GHI).

The different components are described well in Chapter 1 in Kleissl [24], and also described in SolarGis [46]. The two disagree on the abbreviation for Diffuse horizontal irradiance, which is denoted DHI in Kleissl, and DFI in SolarGis. DHI will be used here in accordance with Kleissl. It is important to note that literature describing this is not completely consistent in its terminology, so it is important look up exactly what unit or description is used for the abbreviation in question.

Here follows a short verbal description of each component

- *DNI:* Solar irradiance reaching Earths surface (normal to the sun), without any atmospheric losses due to scattering or absorption.
- *DHI:* Solar irradiance reaching Earths surface after being scattered around in the atmosphere by clouds, aerosols and other particles.
- *GHI:* Is the sum of direct horizontal irradiance (DNI) and diffuse horizontal irradiance (DHI).

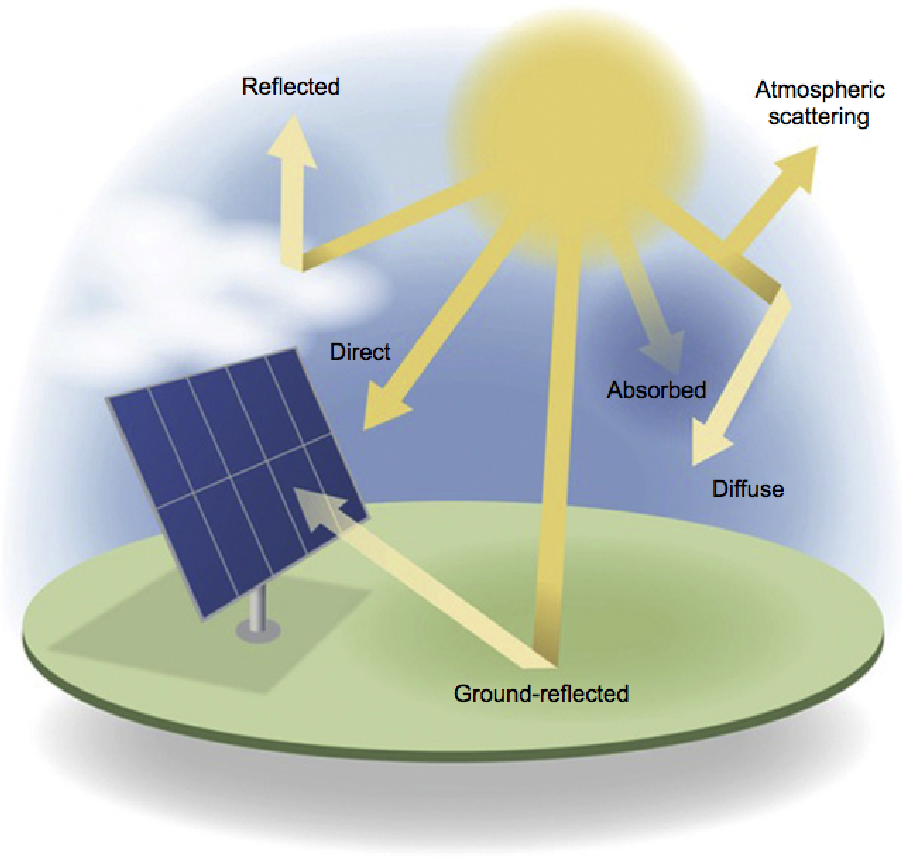

Figure 2.2: Solar-radiation components resulting from refractions in Earth's atmosphere and reflection of the ground. Picture reprinted from Kleissl [24].

Using the solar-zenith angle (SZA) at the time of interest, GHI can be expressed mathematically in Equation 2.3. It is values of GHI which is collected from the respective databases and used for calculations in this thesis.

$$\mathrm{GHI} = \mathrm{DNI} \times \cos(\mathrm{SZA}) + \mathrm{DHI} \tag{2.3}$$

In Figure 2.2 the different solar irradiance components are depicted, giving a visual representation of DNI, DHI and GHI. Also absorbed and reflected light is shown here, which is irradiance that will not contribute to production of energy, as it never reach the PV-panels.

2.2.2 *Satellite measurements*

There are typically two orbits of weather satellites, geostationary orbit and Low Earth Orbit (LEO). Satellites following a geostationary orbit are always perpendicular to the equator, and will, when observed from earth, not appear to be moving at all. It will cover the same area all the time, and deliver data from here. In Chapter 5 in Kleissl [24], it is argued that due to the Earth curvature, the data from geostationary satellites is limited to 60-66° in both northern and southern direction, depicted in Figure 2.3. This is important to remember when collecting data, as it might affect the results considerably. However for the case-study presented in this thesis data will not be affected, as Bhutan is situated between 26-28°N.

Satellites following a Low Earth Orbit (LEO) rotate the earth along the longitudes, crossing the poles, thus also called a polar orbit, with a typical orbiting time of from about 88-115 minutes according to the Australian Space Academy. As the earth spins, this allows the satellite to cover all of earth's surface, which again offers more accurate data on solar irradiance on northern latitudes, as the angle from the satellite to the earth surface remains perpendicular at all times. Both polar- and geostationary orbits are shown in Figure 2.4.

For further explanation and more detailed explanations of earth orbits see NASA Earth Observatory [31].

2.2.2.1 *Meteosat*

European Organisation for the Exploitation of Meteorological Satellites [17] (EUMETSAT) is an intergovernmental organisation, and operates satellites for monitoring weather, climate and the environment.

A part of their programme are the Meteosat satellites, which provide images of the full Earth disc, along with data for weather forecasts. As seen in Figure 2.3, the Meteosat-programme covers much of the European continent, Africa, and large parts of Asia, as well as the Indian ocean. With this coverage, most of the areas affected by the energy poverty mentioned in [21] are covered, making it a viable option for collection of data.

Data can be collected both through their online interactive map-tool [38] and through their Earth Observation Portal.

2.2.2.2 *NASA*

NASAs Atmospheric Science Data Center [3] is responsible for the processing and distribution of the data NASA is collecting worldwide. This also includes both irradiance, and temperature data, which is made freely available to the public.

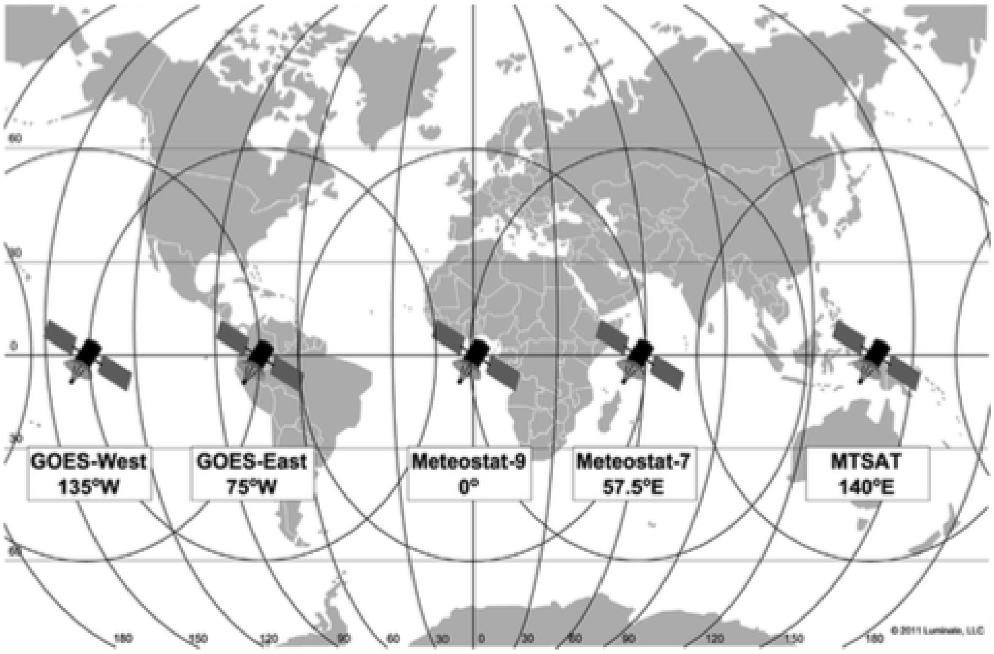

Figure 2.3: Geostationary satellite orbits, including names on certain satellites and their positions. Coverage is also displayed correctly in degrees north and south. Picture reprinted from Kleissl [24].

In their database one can acquire daily insolation values, which must be post-processed to give data with hourly resolution.

The data retrieved is free, and can be obtained to easily fit for different PV-optimization tools, such as HOMER or RET-screen.

2.2.2.3 *Databases*

In Chapter 2.2.2 in Lockertsen [25], several different irradiance databases are mentioned, and evaluated. These includes PVGIS-CMSAF, Meteonorm 7.0, Satel-Light, SolarGIS and NASA/SSE. The findings were that the NASA/SSE - database is the only relatively up-to-date (2005) database which is free and available online. After extensive searching this is also the findings in this thesis. Even though data can be extracted monthly from the map-tool in PVGis, there are no easy ways of collecting a full dataset.

Databases such as Meteonorm 7.0 and SolarGIS have more recent data than NASA/SSE, but require payment in order to supply data.

For further analysis in this thesis, the data from NASAs Atmospheric Science Data Center [3] will be used.

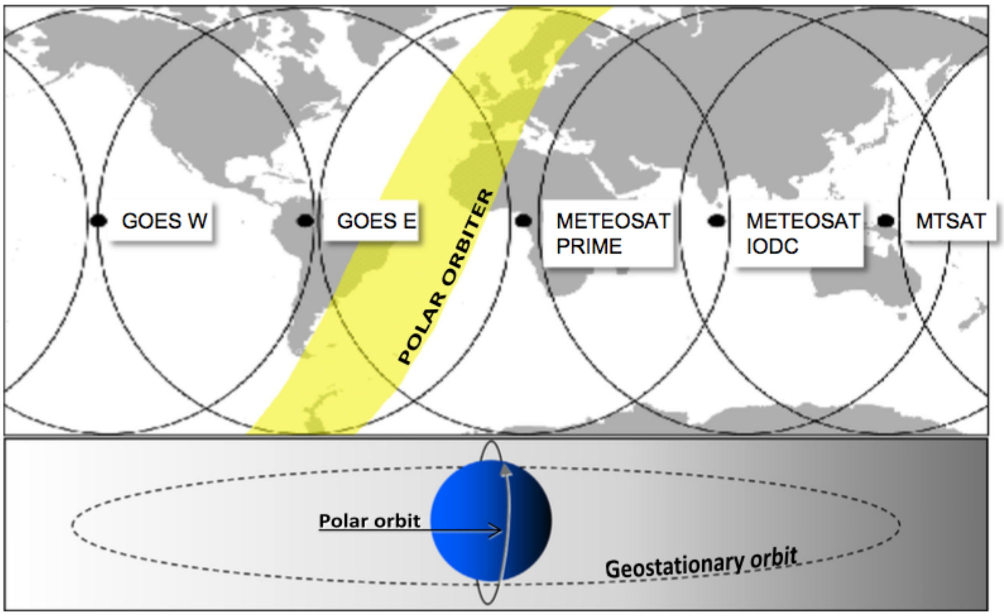

Figure 2.4: Schematic showing the difference between polar and geostationary orbits. A geostationary satellite can give pictures with much shorter time-intervals than polar-orbiting satellites, which only pass over the same place on earth every 88-115 minutes, whereas a geostationary satellite remains fixed over one point at all times. Picture reprinted from Kleissl [24].

2.2.3 *Ground measurements*

Satellite and ground-based measurements have somewhat different uses and purposes. Satellites are used more for long-term studies, such as exploring slow variations in solar resources and finding best suited location for solar facilities. This is augmented very well by the more precise ground measurements, which can be used as an accurate reference point for satellite measurements, as well as measuring short-term variability at a specific site. The relationship is explored more in-depth in Vignola et al. [53].

Whilst ground-measured values are the more accurate ones, it is easy to forget the very real limitations of such measurements. These are well pointed out in Zelenka et al. [57], stating that a site for potential PV-installation more than 25 km away from a ground-measurement device would benefit from using satellite-derived data, as these are more accurate from these distances and beyond from the ground-measurement-device.

Adding that it is beneficial to have long-term measurements (at least a year) to evaluate seasonal changes in irradiance and temperature, satellite-data have a great advantage with decades of available data.

In Gilman et al. [19], the solar potential for Bhutan specifically was evaluated, and it was deemed that satellite-data was sufficient for smaller PV-systems. However, for larger systems, typically several MW, would require a solar resource assessment based on ground measurements. As this thesis is exploring options for rural villages, and primarily smaller installations, this fits well with their recommendation of using satellite measurements. It is also freely available data which is of interest, so unless free solar data is available from local weather-stations, satellite data will be used.

To further strengthen the validity of satellite-derived measurements, two more studies on the matter can be mentioned. One of these were executed at the College of Science and Technology, Phutensholing, Bhutan, the actual site for the case-study in the thesis. The findings in Dolkar et al. [11] where that there only was a deviation of $\pm 10\,\%$ between the satellite- and ground measurements, comparing the data from NASA/SSE-database [3], and local measurements from Department of Energy, Ministry of Economic Affairs in Bhutan. It is to be noted that the measured data is from the year 2012, while the data from NASA was an average over the years 1994-2004.

The second study was conducted by Stein et al. [47]. Here it is pointed out that the ground-measurements give better short-time accuracy, but for longer time-periods as months or years, the estimated power-output from satellite data is very good.

Based on mentioned sources and studies, it is to be assumed that data from satellites provide sufficient accuracy for the dimensioning and optimization on small-scale PV.

2.3 ACQUIRING TEMPERATURE DATA

Power output from solar panels are very much affected by the operating temperature of the cells, and consequently ambient temperature. The relation between ambient and cell temperature is found in Equation 5.7 in Keyhani [22], and is here represented by Equation 2.4:

$$T_{cell} = T_{amb} + \frac{E}{E_{NOCT}} \times (NOCT - T_{amb,NOCT}) \tag{2.4}$$

E	Solar irradiance, $[W/m^2]$
$NOCT$	Nominal Operating Cell Temperature
E_{NOCT}	Standard irradiance, $= 800\ W/m^2$
$T_{amb,NOCT}$	Ambient temperature at NOCT $= 20°C$

Table 2.1: Nominal Operating Cell Temperature and Standard Test Conditions are two different terms used for standard values on the performance of PV-cells.

	NOCT	STC
Irradiance	$800\ W/m^2$	$1000\ W/m^2$
Temperature	47°C	25°C

The NOCT varies between manufacturer, but is typically around 48°C [30],[37].

This cell-temperature is then used for calculating of maximum power it is possible to extract at given temperature, here in a variation of Equation D1 in Mandelli [28]:

$$P_{cell} = P_{STC} \times \frac{E}{E_{STC}} \times \left(1 - \frac{\gamma}{100} \times (T_{cell} - T_{cell,STC})\right) \tag{2.5}$$

STC	Standard Test Conditions
P_{cell}	Power output from the cell, $[W]$
P_{STC}	Rated power of the cell at STC
E_{NOCT}	Standard irradiance, $= 800\ W/m^2$
$T_{cell,STC}$	Ambient temperature at STC $= 25°C$

Where γ is a temperature coefficient of power, and expresses the power deviation to temperature of the cell. This parameter is given by the manufacturer of the specific cell, and is typically $0.35 - 0.45\,\%$ [28].

It is worth noting that there's a distinct difference between NOCT mentioned in Equation 2.4 and STC in Equation 2.5. Referring to the definitions of the two used by Fraunhofer Institute of Solar Energy Systems ISE [18], the differences are represented in Table 2.1.

From Equation 2.5 it is evident that higher temperatures decreases the general efficiency of a solar panel, and colder temperatures will in fact increase the efficiency of the panels. If placed on windy locations, convection will contribute to lower the cell-temperature of the panels. The manner in which the panels are mounted plays an important role here, are they put on the top of a roof, with no room for convection on the back of the panels, or on a free-standing rack that easily allow for wind to pass around the panels?

Another method to lower cell temperature would be to use the excess heat from the panels to heat water, and thus saving energy on hot water, while increasing the efficiency of the PV-panels. A system like this is called PV/thermal system, and a small study is conducted in Dubey et al. [12], showing increased efficiency with lower temperatures.

Seeing that temperature has a high impact on the efficiency of the PV-panels, this parameter is also important to consider when sizing the system. Ambient surface temperature can also be collected from satellites, using the aforementioned databases.

3 CONSUMPTION ASSESSMENT

The shape of a load-profile and what time of the day peak hour occur, is imperative for dimensioning and planning of grids. For islanded grids it is crucial to have some knowledge about this in order to correctly dimension the battery packs to cover for the energy needed if there's a lack of solar resource. Should the peak-load coincide with peak-sun, there is almost no need for backup battery power. If, however, peak-load is at minimum (or no) sun, all the required energy must be stored in batteries. This is costly, and within a set budget frame, an increased battery pack would be on behalf of other components, such as PV-panels. In Figure 3.1 three load-profiles are depicted together with solar irradiation to demonstrate the importance of knowing *when* the peak-hour occurs, to properly optimize the system for the user.

In the following, two possible ways of synthesizing a load-profile will be presented. One analytical model in Matlab, which also employs a certain degree of stochastisity between days, and one simplified model in Excel, which will give the same output for all days. Both these methods will then be applied to the case-study.

Other ways of creating load-curves for a village or domestic installation would be to use data from another village with similar behavioural and working patterns, giving quite a good idea on the load-profiles' shape, and then scale according to population or other parameters which will give an indicator on total energy-consumption. This method will not be presented here, but is only given as an idea for other projects.

Finally, a simple way of adding seasonal variability to the annual load-profile will be presented, in order to make the result somewhat more realistic.

3.1 TOOLS FOR ESTIMATING LOAD-PROFILES

For properly sizing an off-grid system, knowledge to the load, and during what hours the peak load occurs is imperative.

The obvious lack of consumption data in villages yet to have electricity poses a challenge, and thus a load-profile needs to be synthesized. Typical resolution for load-profiles and irradiance-curve in this thesis is one hour.

For both methods presented, a minimum of data must be present. This includes what kind of appliances which are, or will be present in the installation,

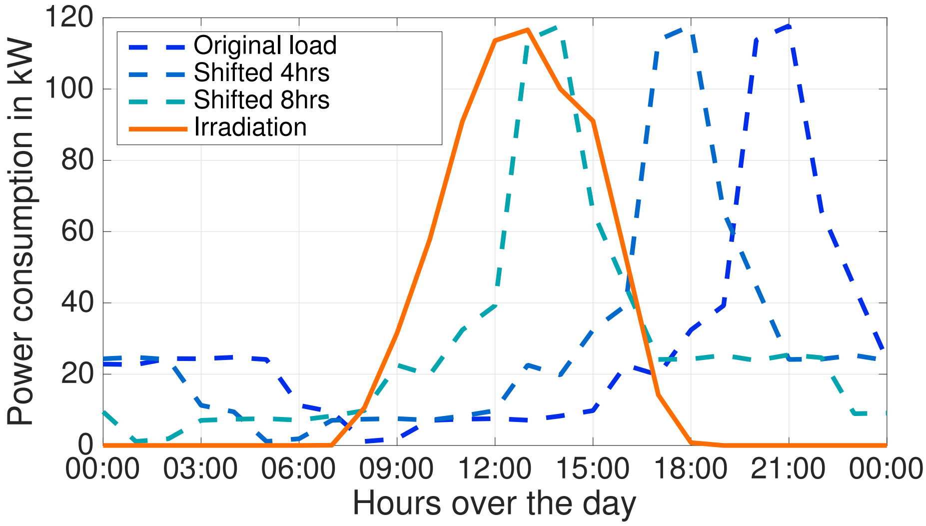

Figure 3.1: Load-profiles shifted from the original with -4 hours and -8 hours depicted together with solar irradiance. It is evident that greater coincidence between irradiation and load reduces the need for battery-storage, and thus decreases system cost.

their rated power, and an approximate time-window of when they will operate.

3.1.1 *Analytical model*

In Mandelli [28] a Matlab model is presented for creating a 24 hour load profile based on the possible electrical applications that are to be expected in a household or other facilities connected to the grid. Each kind of facility is defined as a "user class", and one can thus build up a system consisting of a number of different user-classes, each class having its' own behavioural pattern and different load.

As the load in this case is solely a student hostel, it is assumed that all students behave the same, and thus only one user class will be made here, with its own behavioural pattern.

The model opens for a degree of stochasticity between days. Table 3.1 is a replica of Table 5.1 in Mandelli [28], clearly showing what considerations are made in the production of the load-profile. As seen the different applications can function at somewhat different times every day, but within a given time-window. This makes for a small variation on peak-load between days, depending on the input-size of the random variation. A time-window is the

Table 3.1: This is a reproduction of Table 5.1 in [28], showing what data is required in this procedure of creating a daily load-profile.

N_j	number of users within class j
n_{ij}	number of appliances ij
P_{ij}	nominal power rate [W] of appliance ij
h_{ij}	functioning time [min] or [h], i.e. duration of the period the appliance ij is on in a day
$W_{F,ij}$	functioning window(s), i.e. period(s) during the day when an appliance ij can be on (Figure 3.2). Defined by a starting window time and a ending window time
d_{ij}	functioning cycle [min], i.e. minimum continuous functioning time once appliance ij is on
Rh_{ij}	% random variation of functioning time appliance ij
RW_{ij}	% random variation of functioning window appliance ij

period when a certain appliance is allowed to operate. One appliance can have several time-windows in one day, which is illustrated in Figure 3.2.

A final note is that there is no inbuilt function in this program to create seasonal variability, which is explained in Section 3.3. Seasonal fluctuations in power consumption is quite normal, so this should be considered and accounted for if it is present. A simple method to employ such variation will be presented there.

3.1.2 *Simplified model*

As an alternative to the analytical model in Matlab, a simplified model using Microsoft Excel can be employed. When doing the calculation in Excel, it is a more manual approach, but the principle is similar to the one previously explained. Operating times for each appliance is set up, and the sum of power used at each hour gives the total power consumption for the respective hour.

This is represented in Table 3.2, where the green squares represent operating hours, and the red squares are when the application is off. Summarising the total energy consumed by each application for every hour gives an hourly load-profile.

3.2 ESTIMATION OF LOAD-PROFILE

When estimating the load for a student hostel at the College of Science and Technology in Duus et al. [13] the method in [28] was used. Data on appliances

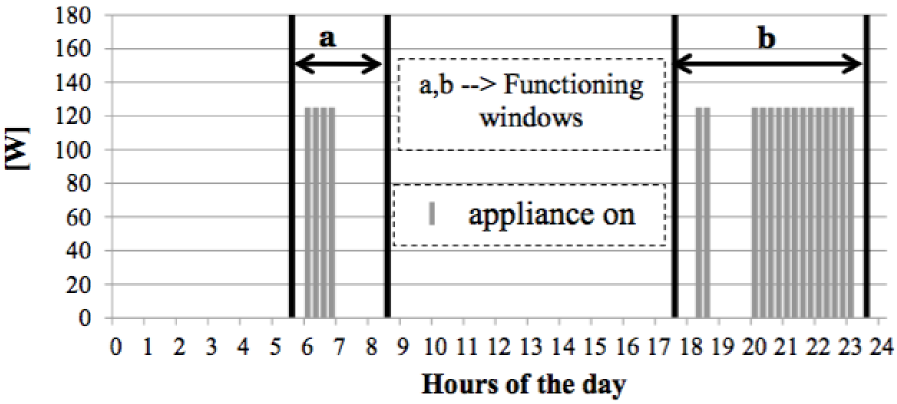

Figure 3.2: Graphical representation of the operating window for an appliance. Replica of Figure 5.7 in Mandelli.

Table 3.2: Simple representation of when appliances are operative. The total load per hour would be the sum of the power of all appliances operating at a given time (marked green). Each square represents two hour of operation.

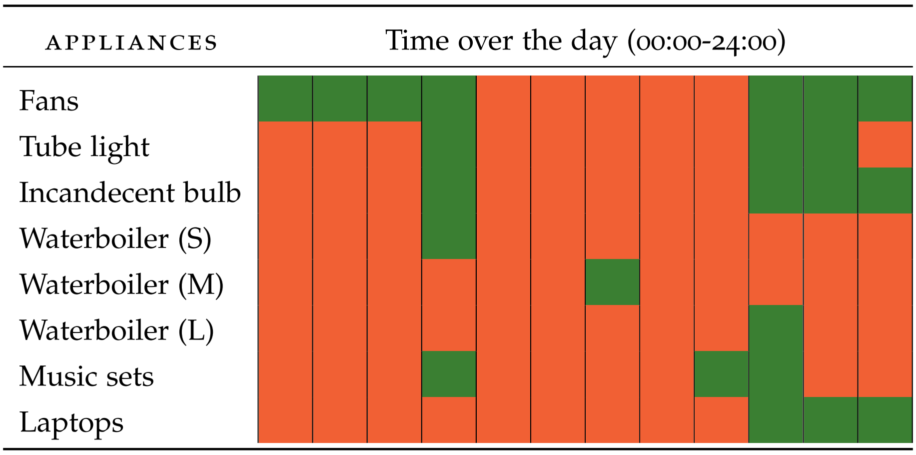

Table 3.3: Overview of appliances and respective energy consumption per day in the student hostel, Block-D. Information was collected by students on-site.

APPLIANCES	#	P [W]	USE [h/day]	E/DAY [kWh]
Fans	41	50	14	28.7
Tube Light	94	40	5	18.8
Incandescent bulb	66	100	5	33.0
Water boiler (small)	12	610	1	7.3
Water boiler (large)	9	670	1	6.0
Water boiler (instant)	5	1500	1	7.5
Music sets	10	30	2	0.6
Laptops	78	55	5	21.5
SUM				**123.4**

present in the hostel Block-D at CST was collected by the students, along with their rated power and use over the day. The collected information is presented in Table 3.3. Also, a very brief survey was done per e-mail to the students at CST-campus as of when they used the different applications.

Available energy consumption data for all respective blocks for half a year was available at the time, shown in Table 3.4.

With the information that there were 41 rooms in Block-D, and assuming that energy-consumption per room is more or less equal, it was possible to estimate the total number of rooms in the hostel-buildings. Making the assumption that appliance-to-room-ratios were equal between all blocks, an expected total number of appliances could be calculated.

This information, along with when during the day appliances are used, were put in to the Matlab-model explained in Section 3.1.1, which then calculated the power consumption at every hour, creating a daily load-profile. The resulting synthesized load profile for the entire hostel complex is depicted in Figure 3.3a, and will be the basis for further analysis in this thesis.

Making 365 "days" like this, and combining them results in a one-year-profile which can be used for dimensioning a PV-system. The yearly profile for the student hostel is depicted in Figure 3.6a.

Using the same data, but applying the simplified model gives a little different result. Taking the operating-hours for each appliance given in Table 3.2, and applying the same methodology as described above to find the total number of appliances results in Figure 3.3b.

Table 3.4: Monthly energy consumption in kWh per hostel-block in 2014. The measuring instrument was installed in mid-April, which is the cause of the low energy consumption this month. Summer holiday is in July, also reducing energy-consumption for this month.

	APR	MAY	JUN	JUL	AUG	SEPT
Dinning hall	329	222	270	63	344	304
Hostel block-A	1480	3200	3680	1760	3400	3280
Hostel block-B	1240	2600	3000	920	2480	2440
Hostel block-C	1240	2600	2800	1000	2440	2640
Hostel block-D	1560	3160	3760	2040	3160	3120
Hostel block-E	1560	3400	4120	1680	3880	3400
RK Hostel LH	960	2480	2800	920	2760	2800
RK Hostel RH	1120	2480	2920	1240	2840	2840
SUM [kWh]	9489	20142	23350	9623	21304	20824

In Figure 3.3 the differences between the analytical and simplified load-models also becomes apparent. It is clearly visible that the load-characteristic of Figure 3.3b is periodic, while Figure 3.3a is aperiodic due to the stochastic approach. The simplified model also produces several hours every day with no-load-situations. In a hostel-complex with 860 residents, this is a fairly unlikely scenario.

This bottom-up approach for estimating load-profiles in rural areas which does not have electricity, is a necessary one, when there are no possibilities of real measurements of consumption. In Section B.2 it will be explored how these assumptions and synthesized load-profile compares with a real measured case.

It is important to mention here that at this point, the authors did not have specific information for each hostel-block, which was the case after the field-trip. As seen in Table 3.4, Block-D has higher energy-consumptions than many of the other buildings, even though it has fewer rooms than both Hostel LH and RH. This caused the assumed number of rooms to be 260 during the calculation of this load-profile, while it in fact should have been 305. It adds to the error of the input-data, and also demonstrates the importance of more local knowledge, as it would've be easy to check the number of rooms in the remaining blocks to get it all correct.

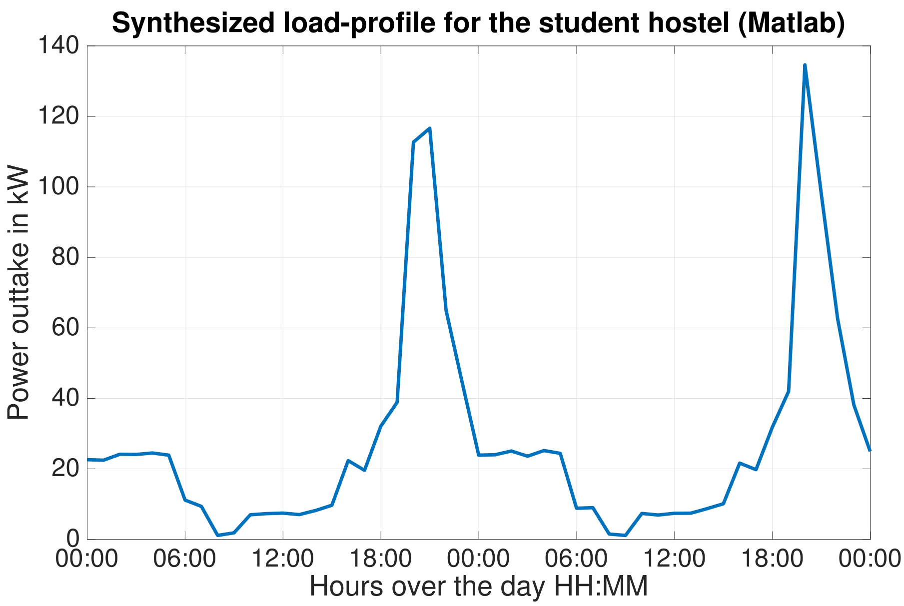

(a) Synthesized with use of Matlab

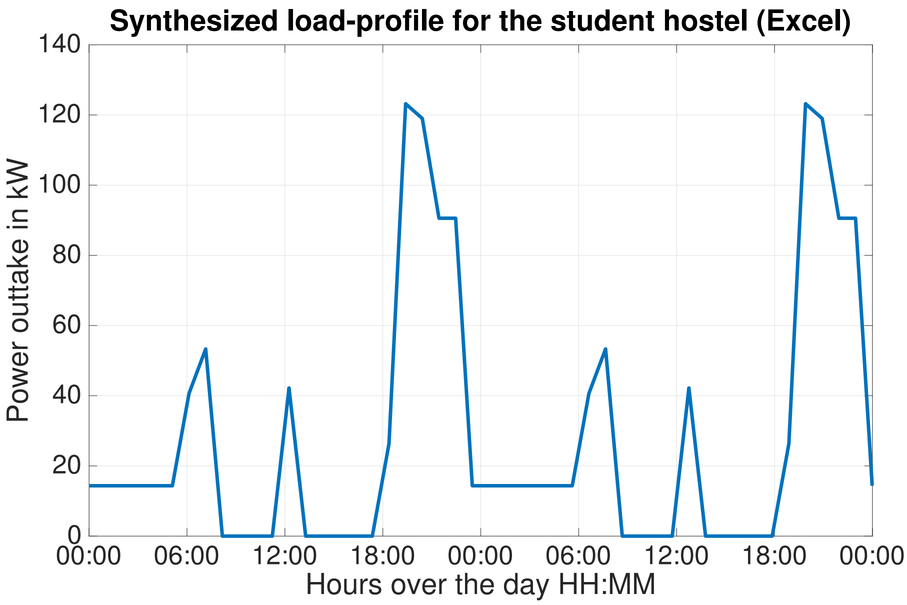

(b) Synthesized with use of Excel

Figure 3.3: Synthesized load for the student hostel, showing load-patterns over one and a half day. The heavy evening-load is due to cooking in the evening, combined with fans during night-time.

3.3 LOAD PROFILE - ANNUAL FEATURES

In most countries around the world, electricity consumption changes over the year according to seasons. Northern countries typically have higher electricity consumption during winter, due to extra need of heating, whereas southern countries usually have a higher consumption during the summer months, when electricity is used for cooling indoor spaces. Data on energy-consumption was collected for European countries and the United States, and is depicted in Figure 3.4. Those countries with typical winter-maxima has been plotted together, and those with summer-maxima has been plotted together, in order more clearly show the trend. Data was collected from European Network of Transmission System Operators for Electricity (ENTSOE) [16].

Here, monthly consumption-data for the years 2012-2014 has been collected, and plotted. In order to make the countries internally comparable, the consumption per month for a given country was divided by the maximal consumption in the current year, expressed in Equation 3.1. Doing the calculations like this gives the maximum month per year a value of 1, and will not show any change of power consumption from year to year. The aim is to show the seasonal variation, not the increase or decline of power consumption.

$$Y_i = \frac{\text{Consumption}_{\text{month,year}}}{\text{Max}(\text{Consumption}_{\text{year}})} \tag{3.1}$$

A simple way to apply seasonal variation is to use sine and cosine-functions, for summer- and winter-peaks respectively. The changes over one year will resemble a half-period of either function. To properly employ this, a reduction-factor R must be set, which will be a measure on the reduction in percent from peak-month to minimum-month. Thus an $R = 0.1$ will represent a 10% reduction of load between the months, which is very little change, and an $R = 0.5$ implies that the consumption is halved from peak- to minimum-month. This is represented mathematically in Equation 3.2

$$\mathtt{Load}_2 = \mathtt{Load}_1. \times [R\sin(x) + (1 - R)] \tag{3.2}$$

R	Reduction factor, R=0.25 equals a 25% reduction in consumption from peak-month to minimum-consumption-month
$\sin(x)$	Half-period of sine-function, where x is a vector ranging [0:π], with equal number of points as $\mathtt{Load}_1$

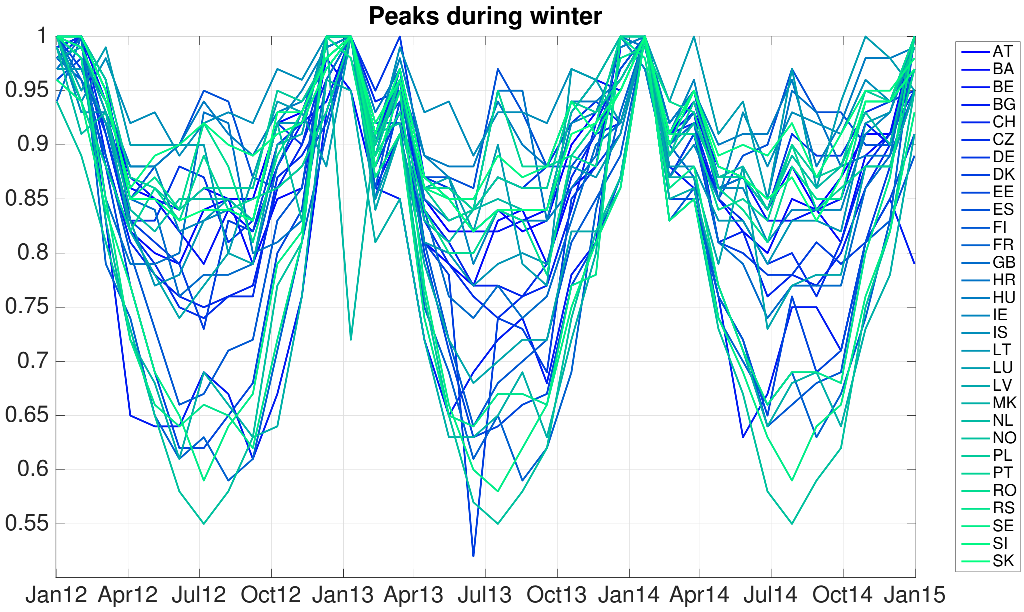

(a) Winter-peaks

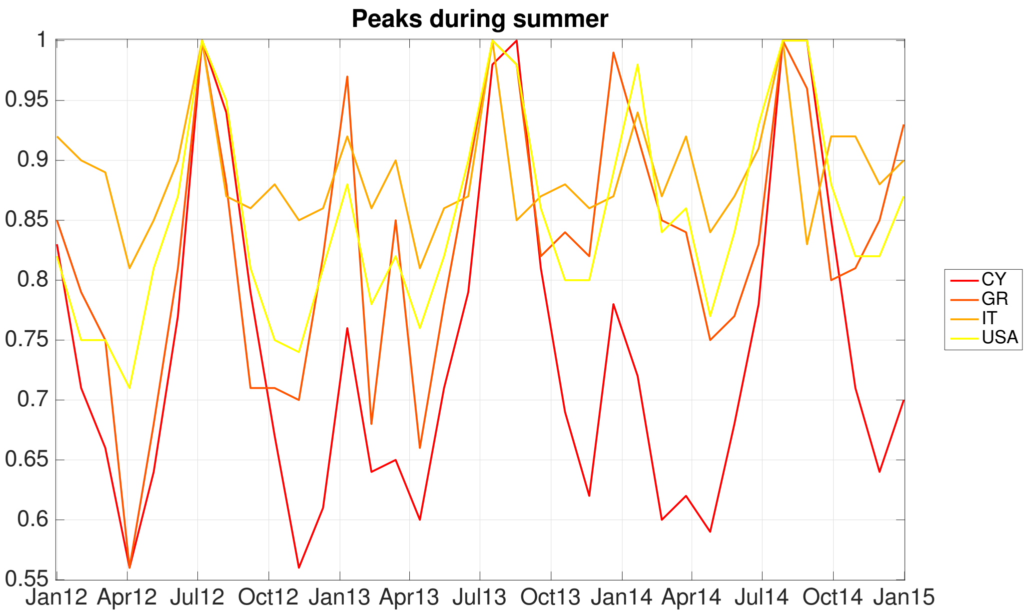

(b) Summer-peaks

Figure 3.4: Seasonal variation over the year is clearly shown here, with some countries having their peak consumption during summer, while most have them during winter season. All countries shown are from Europe, with exempt of United States.

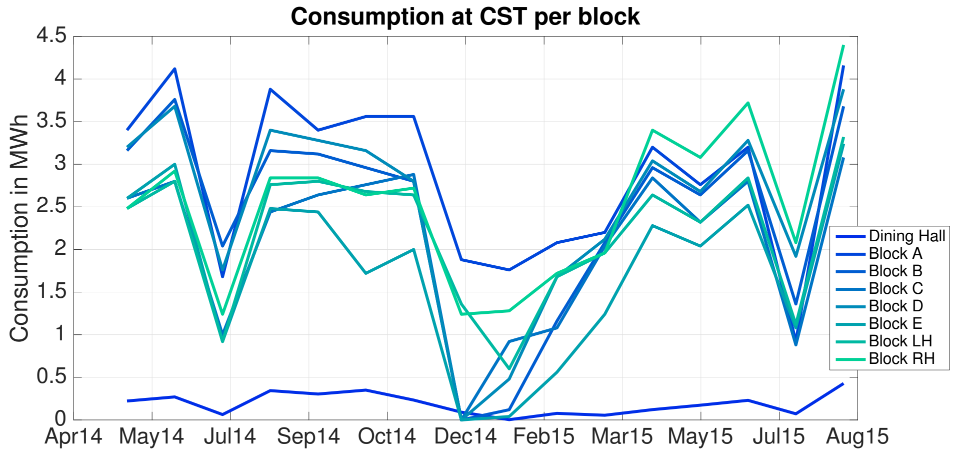

Figure 3.5: Monthly power consumption at CST per block in MWh. Holidays in July and December explain the sudden drop in consumption these months, as students then do not live at the campus during these months.

Employing seasonal variability to an annual load-profile

From Figure 3.5 it is evident that consumption vary by season at the CST, with the maximum peak during the summer, June and August, and at its' minimum in January and February. It is further observed that the power-consumption in February is about half that of June. July and December are excluded from the analysis, as these are vacation months, and will not correctly represent power-consumption of a full hostel.

Having only one year of data, it would be wise to show some modesty, and instead of setting the reduction-factor to 0.5, it should be set to 0.4, which is also within that of several European countries shown in Figure 3.4a. The formula is shown in Equation 3.2. The resulting annual profile, compared to the original without variation, is depicted in Figure 3.6.

This effect was however not investigated in Duus et al. [13], but should be included, as it may have an impact on the optimal system size. Moreover it will be a closer approximation to the real case than having a flat annual load. The effects of seasonal variation on system composition will be examined in Chapter 6.

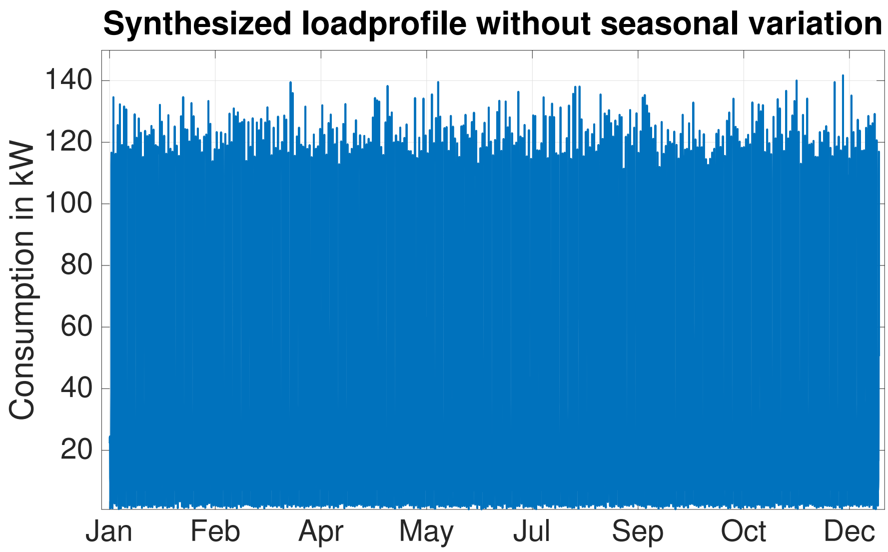

(a) No seasonal variation

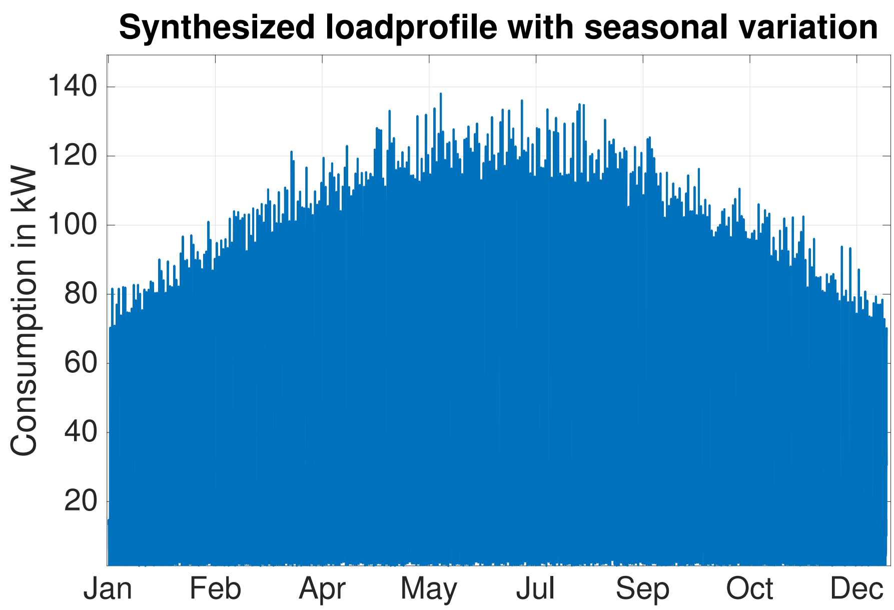

(b) Seasonal variation

Figure 3.6: The original synthesized load-profile from Section 3.2 is shown in Figure 3.6a. Applying the idea of seasonal variation described, results in Figure 3.6b. In this case the reduction factor is 0.4, equalling a 40% load-reduction during winter.

4 INVESTIGATING ECONOMIC FEASIBILITY

In previous chapters, the more technical aspects of system-optimization have been explored. This chapter will investigate the economic feasibility of PV-microgrids.

A typical way of including economics as a parameter, is to use the minimization of life-time costs as objective function. Reduced life-time-costs will impact the price consumers has to pay per unit of electricity, called levelized cost of energy (LCoE). This parameter is represented simply in Equation 4-7 in Short et al. [44], and is given here in Equation 4.1:

$$\mathrm{LCoE} = \frac{\mathrm{TLCC}}{Q} \times \mathrm{UCRF} \tag{4.1}$$

TLCC	Total life-cycle cost
Q	Electric energy output
UCRF	Uniform Capital Recovery Factor = $\frac{i(1+i)^n}{(1+i)^n-1}$, where i is interest rate and n is number of years.

Reducing the electricity price for the customers, especially in rural areas, is of great importance. Thus utilizing an optimization algorithm which does exactly this is quite appropriate.

In the following, parameters of economic nature will be included in the objective function for optimization, with the purpose of minimizing LCoE.

4.1 LOSS OF LOAD PROBABILITY AS RELIABILITY PARAMETER

Optimally sizing a stand-alone microgrid is ultimately a question of balancing system reliability and cost. In the review of sizing-methods in Khatib et al. [23] this also becomes clear, regardless of the sizing-method employed, with the exempt of the intuitive method presented.

When identifying system reliability, this can be done with Loss of Load Probability (LLP) (Equation 4.2). The size of LLP is in the end a question of investment in the grid, where larger investments gives a more reliable grid. This is presented in Duus et al. [13] (Figure 4.1), and also the findings in Mandelli [28] and Celik [8].

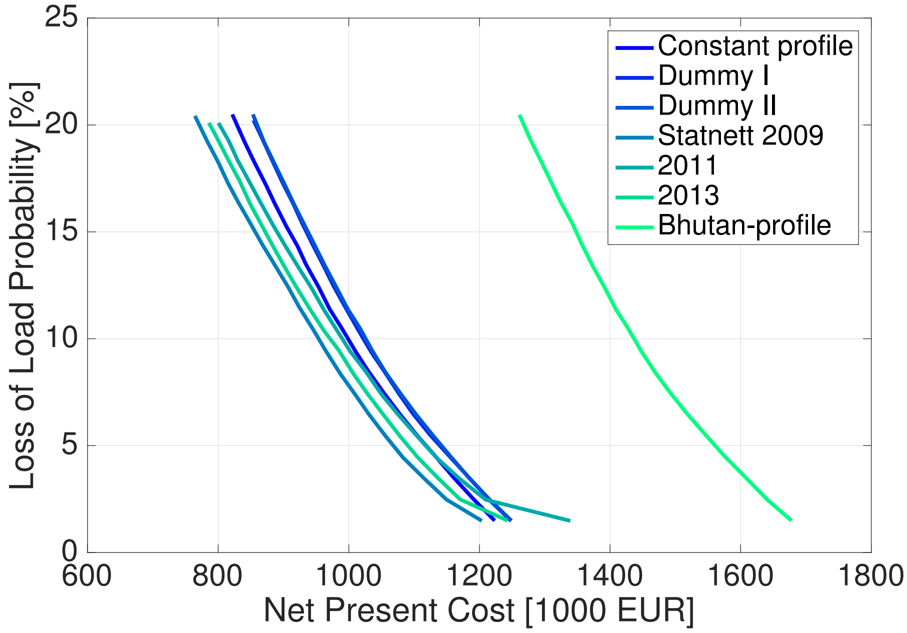

Figure 4.1: This figure shows that increasing system reliability (decreasing LLP) will lead to an increase in system cost. Reprinted from Duus et al. [13].

$$\mathrm{LLP} = \frac{\sum_{t=1}^{T} \mathrm{LL}(t)}{E_{D,T}} \tag{4.2}$$

$\mathrm{LL}(t)$ Lost load at instance t

$E_{D,T}$ Electricity demand for the period T

At the present time, no good analytical method exist to determine what LLP which would be acceptable for a system. Setting an acceptable LLP is ultimately a question which has to be posed to the consumers. What amount of outages are tolerable, and what are they willing to pay to avoid outages?

In order to give some frames on what one could expect from a power-system, some data from both national grid and islanded systems will be presented. Firstly the national grids of Europe will be evaluated.

National electricity grids in Europe have a very high degree of reliability, with low annual downtime. A measure for this is System Average Interruption Duration Index (SAIDI), and SAIDI-statistics for most European countries is presented in Council of European Energy Regulators (CEER) [10]. Almost all countries have less than 0.11 % annual downtime.

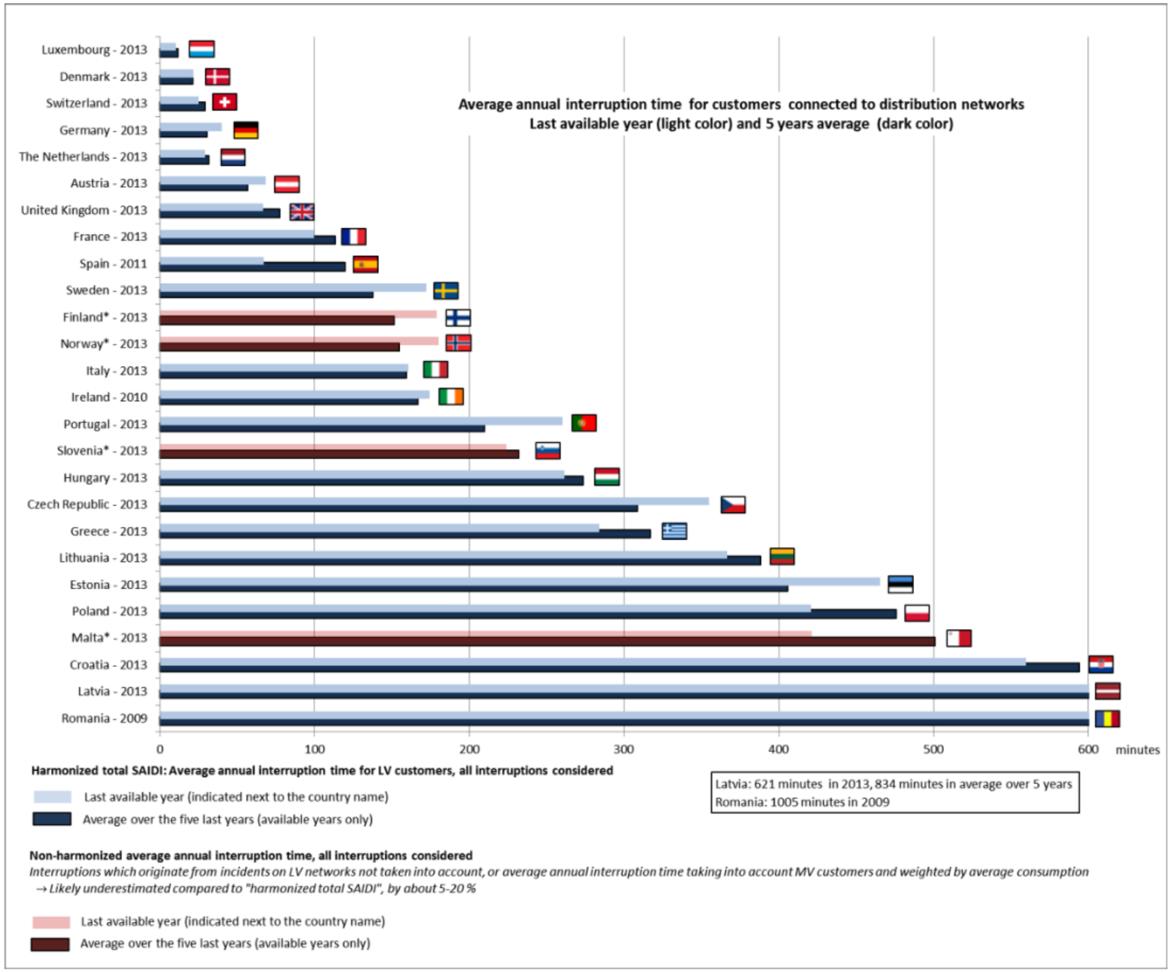

Figure 4.2: 5-year average SAIDI, from 2009 up to and including 2013. Almost all countries have a SAIDI less than 600 minutes = 10 hours per year. This gives an annual system downtime 0.11 %. Reprint of Figure 4 in Council of European Energy Regulators (CEER) [10].

Looking at the mentioned findings that increased reliability exponentially increases system cost, it would seem improbable that such a high degree of reliability would be the best solution for islanded systems in rural areas, with limited investment capital. The system should thus be designed with a higher benchmark LLP.

An example or a rural electrification programme in India is found in Loka et al. [26], which is closer to the target group of this thesis. The system in question is designed with an expected maximum annual capacity shortage of 8 %. In Abdilahi et al. [2] a hybrid system with a wind-turbine, diesel-generator and PV-panels is simulated, with a designed annual capacity shortage of 10 %. Here we have two systems closer to the target group in this thesis, both dimensioning for a much higher annual capacity shortage than seen in the European grids.

As commented in the latter paper, this high annual shortage is not considered harmful for the system, as it is only serving residential loads. And here is the key-point; what kind of load which is served. Is it industrial consumers, hospitals or other critical infrastructure, or residential loads, and what impact will a power-outage have on them?

Returning to the initial question "What are they [consumers] willing to pay to avoid outages?". This is a very quantifiable parameter, which can be included in the objective function when optimizing the grid, and will be explored further in the following.

Cost of Energy not Supplied (CENS)

Closely related to the LLP of a system, is the term Value of Lost Load (VOLL). As electric energy has a value, not only as a commodity, but also as a resource assisting in social welfare, the lack of energy has a cost for the society, and the persons affected by power-shortage. According to Welle and Zwaan [54] VOLL is

> usually expressed in terms of the estimated total damage caused by not delivered electricity, divided by the amount of electricity not delivered in kWh.

Damage in today's society is typically measured in money, whether it be material damage, or loss of production due to power-outage. Using euro as currency, this gives VOLL the unit of $€/kWh$.

Cost of Energy not Supplied (CENS) is directly linked with the loss of load, and attempts to price VOLL for different consumer groups. In Norway, CENS is used as an economic incentive for correct distribution of resources by the utility, and the idea is that at some point it will be more feasible to invest in increased reliability than paying CENS. The grid-regulator is in charge of enforcing this law within the given framework, some of which is presented in Aabakken et al. [1]. If there is a power-outage, the utility will have to pay for this, in accordance with the set rates for the respective consumer groups. For instance an aluminium factory will have much higher VOLL, and consequently CENS, than a domestic household due to losses in production of aluminium during the outage, and possibly fatal damage to equipment.

The full details of rates and correction-factors are found at Olje- og energidepartementet [33]. It must be emphasized that these are rates and considerations for a developed country with a highly reliable electricity grid, and a strong regulating electric authority, and that the purpose of bringing in this information is for the reader to be aware of, and evaluate, the costs of LLP. Of course this must be adapted to local conditions.

With this in mind, it is evident that the optimizing objective function should include some kind of penalty for power-outages, the simplest being a fixed cost per kWh of electricity which is not supplied to the consumer.

4.2 EVALUATING SYSTEM NET PRESENT COST

The system cost is commonly identified by Net Present Cost (NPC), and it is defined as the present value of the sum of the costs for a system over its lifetime. This would typically be represented by Equation 4.3

$$NPC = \sum_{y=1}^{LT} \frac{Invest(y) + O\&M(y)}{(1+r)^y} \tag{4.3}$$

$(1+r)^y$	Discount factor of year y
LT	System lifetime in years
$Invest(y)$	Investment and replacement cost in year y
$O\&M(y)$	Operation and maintenance cost in year y

As seen, this definition of NPC does not concider the LLP or VOLL which was discussed earlier. In order to include these parameters in the novel sizing method, and to give a more complete picture of the total NPC over system lifetime, the modified NPC-expression becomes

$$NPC^* = \sum_{y=1}^{LT} \frac{Invest(y) + O\&M(y) + \sum_{t=1}^{T} LL(t) * VOLL}{(1+r)^y} \tag{4.4}$$

$LL(t)$	Lost Load at instance t
$VOLL$	Economic value of lost load

Equation 4.4 and Equation 4.3 is derived in Mandelli [28], Chapter 7, which also includes a more extensive commentary and evaluation of the different aspects. However this will not be covered further in this thesis, as it is only presenting the novel sizing methodology.

5 OPTIMIZATION TOOLS

There are numerous different optimization tools for PV-systems, and hybrid-systems, all with their own speciality and core-functions. The most extensive list found in the litterature review for this thesis is Connolly et al. [9], which compares 37 different computer tools for renewable energy systems. This study can be used as a small guide to which tool is best suited for the respective purpose, as they all have their specialities for different scenarios. Furthermore, it contains several references to cases where the respective tools have been utilized. In addition, a shorter list is found online at Photovoltaic Software [34]. This second list contains somewhat different tools.

In the following, a small selection of such tools will be presented and commented. These have all been tested and used as a part of the ground-work for this thesis. Finally some general comments will be made, and the advantages of the novel-sizing methodology over the already available tools will be presented. As some of the emphasis in this thesis is in accessibility for everyone, the optimization-programmes should be free, and not add to system cost. Consequently, all testing of programmes has been done utilizing their free-trials or the like, if they do not give full-versions for free.

Most of the background material for the comments has been researched by Lozé [27] and Sakepa [42] during a summer-internship at NTNU in 2015.

5.1 EXISTING OPTIMIZATION TOOLS

5.1.1 *HOMER*

Hybrid Optimization of Multiple Energy Resources (HOMER) is a widely used tool for the optimization of microgrids, a few examples of this is found in [56], [2] and [11]. The software is developed by the National Renewable Energy Laboratory (NREL) and is freely available for download at HOMER Energy [20].

During a summer-internship in 2015 at NTNU, Anne Lozé extensively tested HOMER, and how it behaved under different circumstances. A full report for internal use was written, and is presented in Lozé [27].

The findings were that HOMER is a flexible tool when a project is set in a location, and prices are either set, or known in advance. There are also good options for hybrid systems, as shown in [56]. Furthermore, the economic analysis can be quite good, if necessary parameters are known in advance, such as inflation-rate, salvage cost etc.

However, there are things which makes it inflexible and somewhat difficult. To begin with, PV and batteries are predefined, and will be added to the system in user-defined strings. It is not certain that the optimal system size will be in steps of these strings, it could lie between.

The budget used for the optimal system is also infinite, which is seldom the case when building microgrids. It should be possible to set a budget-constraint for the system.

Also, some enigmatic behaviour was observed during the testing, such as two simulations ran with the same input, would result in different optimal solutions. It would also be observed that during periods of lost load, the batteries were not discharged to minimum allowed state of charge. In other words, one would experience loss of load, while still having capacity left in the system.

As a last remark, it was tested if system-composition would change with different timing of peak-load, as explained in Chapter 3. The initial findings were that system-composition in fact did *not* change, contrary to what is to be expected. However, further analysis is needed in order to fully verify of this is indeed true.

5.1.2 *BlueSol*

As explained in the introductory, only free programs, or trial versions were tested. BlueSol is a technical program which requires a licence in order to access the full program, resulting in that only the trial version was tested in this study. For reference, their software costs 290 € and 490 € + VAT for the two versions. This would be significant extra cost for a domestic system which could buy 1 kW of PV for about 1000 €.

BlueSol is developed by CadWare, and is available for download at their homepage BlueSol [7].

This program is more technical then HOMER, and opens up to perform the entire process of PV-system design. It has data from every country in the world, but for Bhutan it can only acquire data from Thimphu, which is quite inaccurate when the system being evaluated is in Phuentsholing. This is a major drawback, as one can not enter user-specific data.

With only the trial version available, it is only possible to add PV-panels to the system, leaving out the critical batteries, and giving an incomplete system as output.

With its full version, BlueSol might be a good program with many technical specifications and options, but as a free tool, it is way to limited to be of any proper use.

5.1.3 *RETScreen*

RETScreen International [41] is an Excel-based optimization-tool, which is also widely utilized worldwide. There are good options for a detailed economic study, but was lacking in flexibility when it comes to simulating the system power-flow. E.g. it was not possible to differentiate between seasons when the consumption-profile was imported to the system. This is something which could affect the system composition, but is not considered in RETScreen.

As is noted in Connolly et al. [9], RETScreens fundamental function is the comparison between a 'base case' and a 'proposed case', typically being conventional and clean energy technology respectively.

5.1.4 *PVSyst*

PVSyst [39] is more directed towards the sizing and data analysis of complete PV system than RETScreen, with options for both grid-connected and standalone PV systems. Furthermore, it includes extensive meteorological and PV-systems-components databases.

The preliminary design option allows you to choose which kind of system is desired, along with a specified location. It uses monthly meteorological values to perform a quick evaluation of system, and set up an optimal system for the site. Losses in converters, inverters and heat, amongst others, are also evaluated.

A study executed by Siraki and Pillay [45] compares PVSyst with Ecotect, and deems PVSyst to be a detailed tool, which might be better suited to use in the detail design phase, and not for the initial planning. It also lacks a load-flow model.

5.1.5 *RAPSim*

The Microgrid Simulation tool RAPSim described in Pöchacker et al. [35] was not tested during mentioned summer-internship by either Lozé or Sakepa, but must still be mentioned here. This tool attempts to do something of similar regard to what is explained in this thesis, namely creating an opensource software for microgrid simulation.

It points out the lack of possibilities to run powerflow calculations in already existing softwares, and aims to create a new tool to do exactly this.

The paper presented also contains a small case-study to show the use of the software, with powerflow-analysis, a description of available tools and modelling, along with climate and weather-simulations.

Some shortcomings of this software, in comparison to the one presented in this thesis, is the lack of mentioned "full-path-coverage". To the best of the authors knowledge, RAPSim neither makes a detailed optimization-scheme for the system, nor an economic analysis. These are both things that is needed for a complete software.

5.1.6 *The novel sizing methodology*

The tool used as basis of the calculations done in Duus et al. [13] was created by Stefano Mandelli, and is thoroughly explained in Mandelli [28].

This tool is specifically designed for optimizing grids in rural areas, and attempts to minimize the NPC of the system. NPC greatly affects the price of the energy, which is important to keep as low as possible when designing for low-income areas.

As it is developed with rural areas in mind, the amount of input data is kept to a strict minimum, just including load-profile, irradiance- and temperature-data, plus cost of PV-panels and inverter in €/kW and battery-cost in €/kWh. Which currency that is used is of course optional, the currency in will be the currency out. It is thus also easy to adapt to local conditions and prices directly, without having to convert between different currencies.

Furthermore, it is open-source, enabling all users to improve, change or redefine everything to accommodate their desires. This is also valuable if anyone would investigate more specifically how optimization is done, what base assumptions are made, and how it will impact the system. In Duus et al. [13] this was exploited in order to compare a multitude of system at once, with different annual loads, or load-profiles. An otherwise tedious task in closed source programs which have no specific option to do this.

Added to the original work in Mandelli [28] is the visualisation of annual production, flexibility in creating a load-profile, along with the 24 hour Simulink-model for more detailed system analysis. With these extensions, a tool covering the full system-path does now exist, and can be used for system-optimization and evaluation.

Some criticism to this methodology is that it's based in Matlab/Simulink, which are not free programs. However, the optimization-code can easily be translated to Python, and alternatives to Simulink exist in programs such as MapleSim and SystemModeler.

5.2 CONCLUDING REMARKS - OPTIMIZATION TOOLS

Danielle Sakepa tested both PVSyst and RETScreen and found that they augment each other well and can be used in conjunction, in order to both get a good idea on system sizing and optimization in addition to the economic analysis. Adding the power-flow-analysis from RAPSim would make the system-analysis even more complete.

HOMER, which is often described as the leading software on microgrid-optimization, has several shortcomings comparing to some of the other softwares mentioned here. The most obvious being the lack of proper power-flow analysis, and being a closedsource software.

The novel methodology for sizing and optimizing microgrids should thus include elements from all mentioned softwares here. Typical properties would be:

- The estimation of a load-profile
- Economic analysis of system components and composition
- Optimal sizing of system components
- Detailed power-flow simulations, both in long-term and short-term
- Based on an opensource platform

All these properties are covered in the methodology explained, and in the following chapters this methodology will be used for dimensioning, optimizing and studying an islanded PV/battery-system.

6 ANALYSIS OF DESIGNED SYSTEM

Utilizing the software initially created by Mandelli [28] and described in Section 5.1.6, with given inputs of solar-irradiance, ambient temperature and load, an optimized system size is estimated.

In the following, two solutions will be presented. One with a "flat" annual load, meaning there will be no seasonal variation, and one system with applied seasonal variation, as described in Section 3.3, and employed using Equation 3.2.

6.1 EVALUATION AND CLARIFICATION OF INPUT DATA

The daily load-profile used for the optimization is that depicted in Figure 3.3. It is important to emphasize that it's the characteristics of this profile which will be the same over the year, as the daily energy consumption will vary to some extent. More so for the system with the applied seasonal variation.

Additionally, for both seasonal and no seasonal variation, a second load-profile derived from the measured consumption-values during the field-trip in September-October 2015 will be used for system-optimization. The purpose of this is to investigate how much impact detailed local knowledge will have on system-composition. Seasonal variation for this system will be employed utilizing monthly measured data in Table B.1, multiplying each month in the load-profile with the normalized monthly consumption over the year.

Annual energy for all annual profiles both with and without seasonal variation is based on meter-reading from the CST, from May 2014 until, and including April 2015, totalling 188 653 kWh. The resulting load-profiles are shown in Figure 6.2, both with daily profiles, and for a full year, then with seasonal variation. On a first look, it appears that they are of unequal annual consumption, however a closer look reveals that the measured profile has a much higher baseload than the estimated profile, which covers for the extreme night-peak found in the synthesized profile.

6.1.1 *Verification of solar-data*

In Section 2.2.2 it was argued that satellite-data could be used for the optimization-process. A weather-station was installed at CST in January 2015, so it was possible to compare actual measured solar data with satellite-collected data.

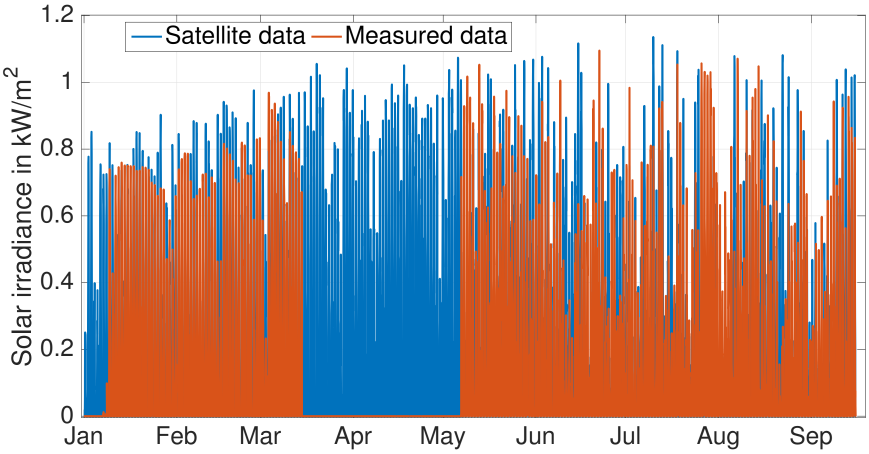

Figure 6.1: Solar irradiance measured from satellites in 2004 (blue) plotted together with actual ground-measurements (red) taken from January until mid-September 2015. The lacking data in April from the ground-measurements are clearly visible.

The available data from the weather-station start 07.01.2015 until 14.09.2015, with an unfortunate loss of data from the last half of March until the beginning of May. Now, plotting together the input irradiance data used in Chapter 6 with that measured at the CST, results in Figure 6.1. The lacking data from the weather-station is clearly visible in the figure.

Comparing total energy from the two measurements during the period both were operative, reveal that the satellite measurements show 17 % more energy than that actually measured on ground.

Looking at Figure 6.3a, and comparing annual insolation between the years, there is a deviation of $\approx \pm 3\%$ from 2004 to the other extremities. Thus, it is not possible to say that the large deviation between satellite-data and ground-measured data is caused by seasonal variations alone, there is clearly a measurement error. This error is however in accordance with the uncertainties presented in Zelenka et al. [57] and by NASA Atmospheric Science Data Center [3] which ranges from 10-30 %, increasing with latitude.

It must be assumed that the ground-measurements indeed are the most accurate. In this case the system designed would also produce less energy than expected, as the irradiation on-site is lower in reality than estimated.

Alas, there is not one full-year measurement of irradiance from CST, and the satellite-data will have to do. The information provided by the comparison should still be kept in mind however, and actual LLP for the system should be expected to be higher than estimated.

Table 6.1: Assumed component costs for system optimization.

COMPONENT	NOTE	Cost	
PV panels	Monocrystalline	1000	€/kW
Batteries	Lead acid	140	€/kWh
Inverter		500	€/kW
Other expenditures		20	%
Operation & maintenance		50	€/kW/year
Plant lifetime		20	years

To see the data used for optimization in context with other years, data back to 1995 was retrieved from mentioned database, and was all set in the same plot, depicted in Figure 6.3. Both for temperature- and solar-data the year 2004 was used, and it is highlighted in red in the plots. As it appears in the figure, the year 2004 does not really stick out, and is deemed to be representative enough for basis in the optimization process.

6.1.2 *Economic variables*

In order to find the NPC for the system, prices on the individual system-components must be set.

The prices for individual system components are shown in Table 6.1.

PV-panels was set to a general 1000 €/kW according to Fraunhofer Institute of Solar Energy Systems ISE [18], and the prices of inverter and batteries were acquired from MCM Energy Lab in Milano by Mandelli.

Lead-acid batteries are chosen due to their low price/kWh, as well as their ability for deep-charge cycles, down to 20 % SoC.

6.2 SYSTEM COMPARISON AND CONCLUSIONS

Running the optimization-code for system composition for the four different cases gives optimal systems for respective dimensioning LLP, along with information such as investment-cost, NPC, levelized cost of energy and investment cost. Much of the data which is produced will not be presented here, as the aim here merely is to present the novel optimization methodology, and not to run detailed economic analysis.

A full overview of system composition for all LLPs for the four different cases is shown in Table 6.2, whereas Figure 6.4 gives a graphical representation

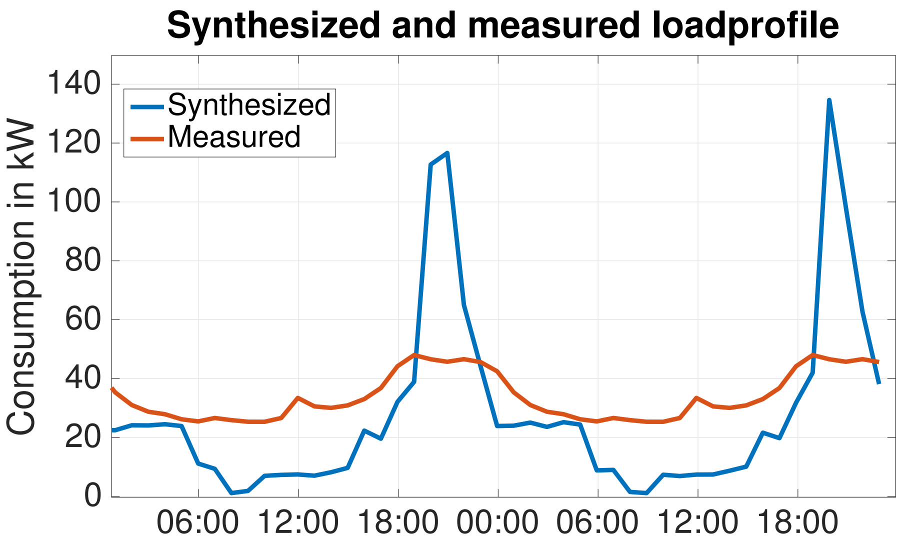

(a) Both load-profiles shown together for maximum month

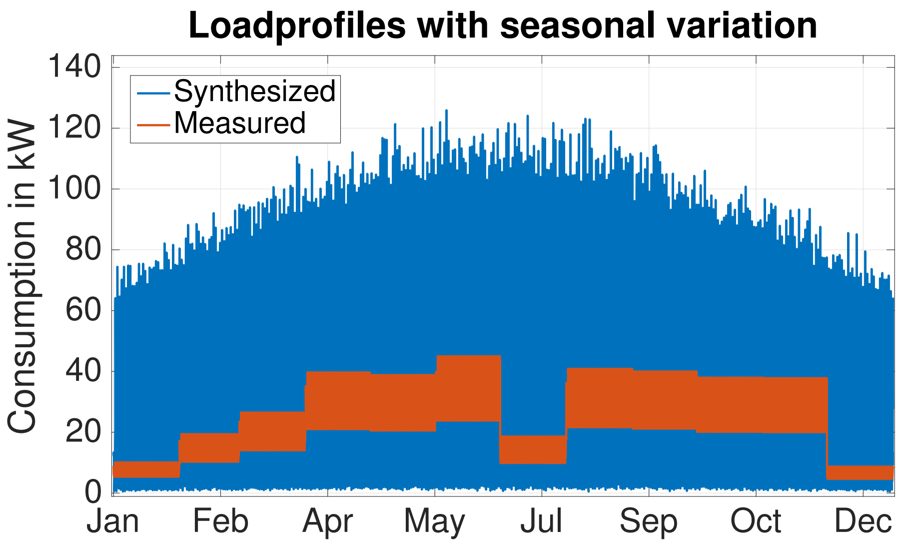

(b) Load-profiles shown together with seasonal variation

Figure 6.2: Comparing the synthesized load-profile (blue) with the measured load-profile(red). The stepwise seasonal change for the measured load-profile in Figure 6.2b is caused by the implementation, using normalized monthly consumption over the year as a correction-factor. A fully real case would of course have more gradual changes between the months.

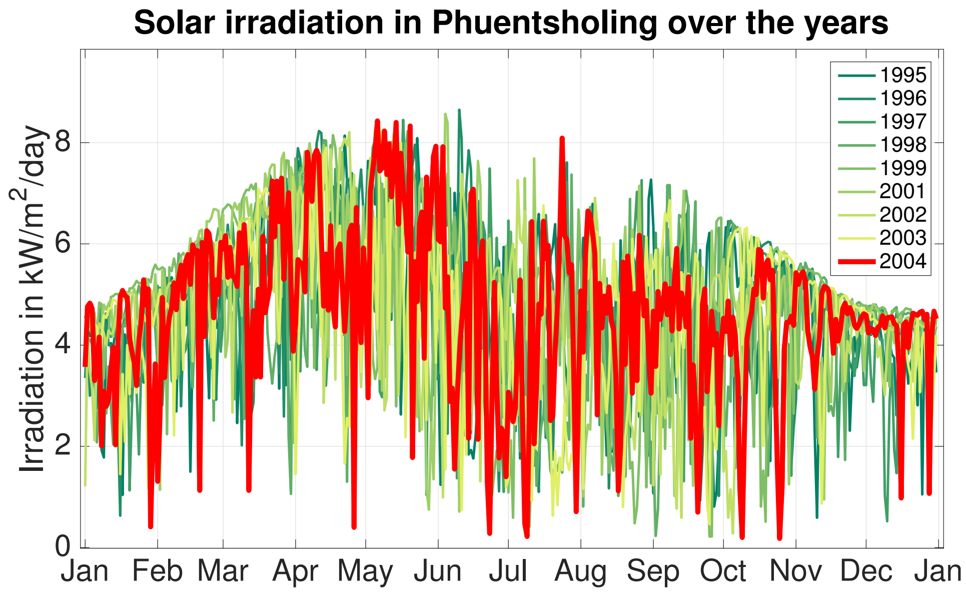

(a) Average solar insolation on horizontal surface in kWh/m^2/day

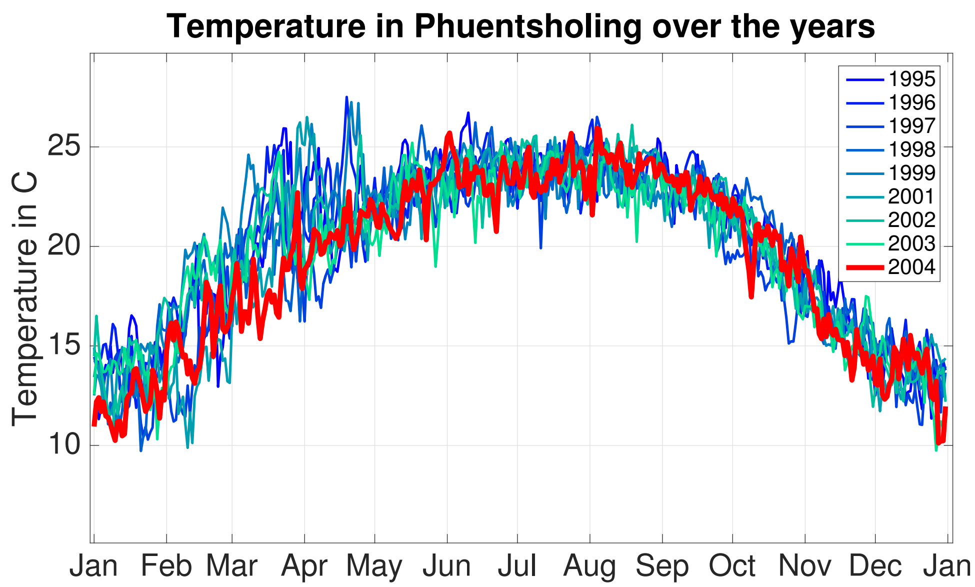

(b) Average earth skin temperature in °C

Figure 6.3: Plotted weather-data from NASAs database EOSWEB for the area of Phuentsholing, Bhutan. The data utilized for the system optimization is that of 2004, marked red in the plots. The years 1995-2003 are plotted together here in order to give a sense of what is normal, and what is to be expected.

of the results. One of the first things to be noticed is that reliability in the sense of low LLP comes with a price-tag. Investment cost increases exponentially as reliability improves. Another attempt to show why it increases so much is given in Figure 6.4b. It depicts the ratio of battery-size to PV-size. The relation between the two is more or less the same, down until about 5 % LLP. Here the battery size increases much more than that of PV, in order to accommodate for the increased need in reliability.

With this as a preliminary result, it could be argued that dimensioning a microgrid with an LLP of no less than 5 % might be a good idea, given that it is not to serve any critical loads, as described in Section 4.1. This will ensure that more of the investment goes to PV-panels, which actually produce energy. Further increasing system reliability is mainly a question of battery-packs, which could easily be added later on, should the consumers be very unhappy with the current conditions.

Examples of systems with this high, and higher LLP has been discussed in earlier chapters, without any arguments behind the reasoning for these dimensioning parameters. Looking at the data from the novel sizing methodology, an initial framework for determining LLP can be developed, not only on what is acceptable for the consumers, but also to some extent on what is "smart" use of money.

Following this reasoning, the optimal system with LLP of 5.5 % will be used for further analysis in Chapter 7, and it is the systems with seasonal variation which will be evaluated. Looking at system composition for the profiles with seasonal variation, they are found to be more or less the same, and thus only the measured case with seasonal variation will be evaluated, with a system composition of 280 kW PV and 985 kWh of batteries.

It is interesting to see that the systems are relatively close to each other both in respect to system composition, but also in NPC. Looking at Figure 4.1 reveals that systems with same annual energy, but with different load-profiles can differ much in terms of investment-cost. Looking at Figure 6.4a it is seen that the investment-cost of the synthesized system is a steady $\approx 10\%$ higher than for the measured case, and that it is in fact the same for low LLPs. It is a small confirmation that it is possible to do preliminary assumptions that are not completely off from the real thing, given that only some basic information is provided.

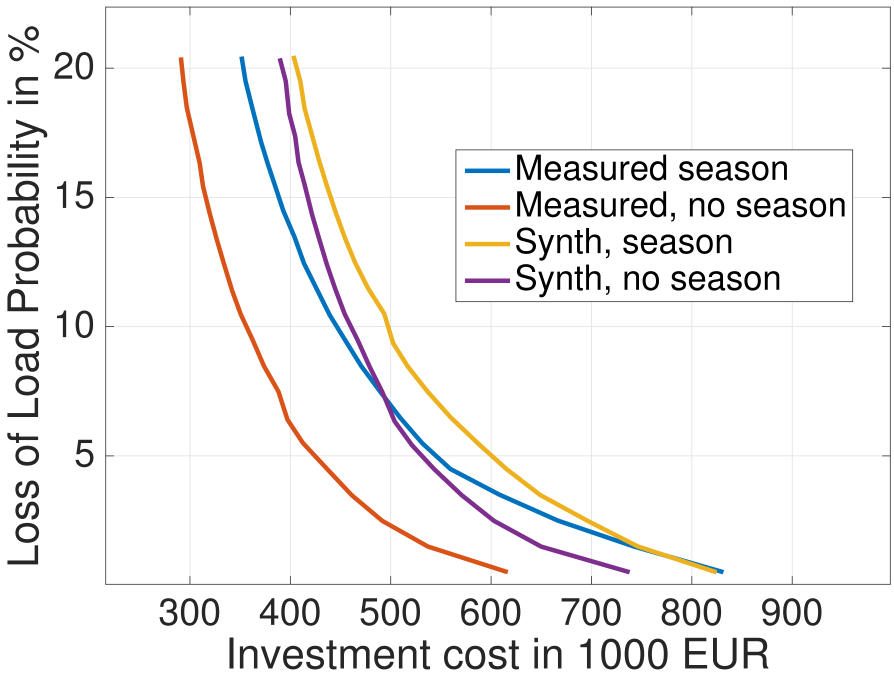

(a) Loss of Load Probability to Investment Cost plotted for the four different cases

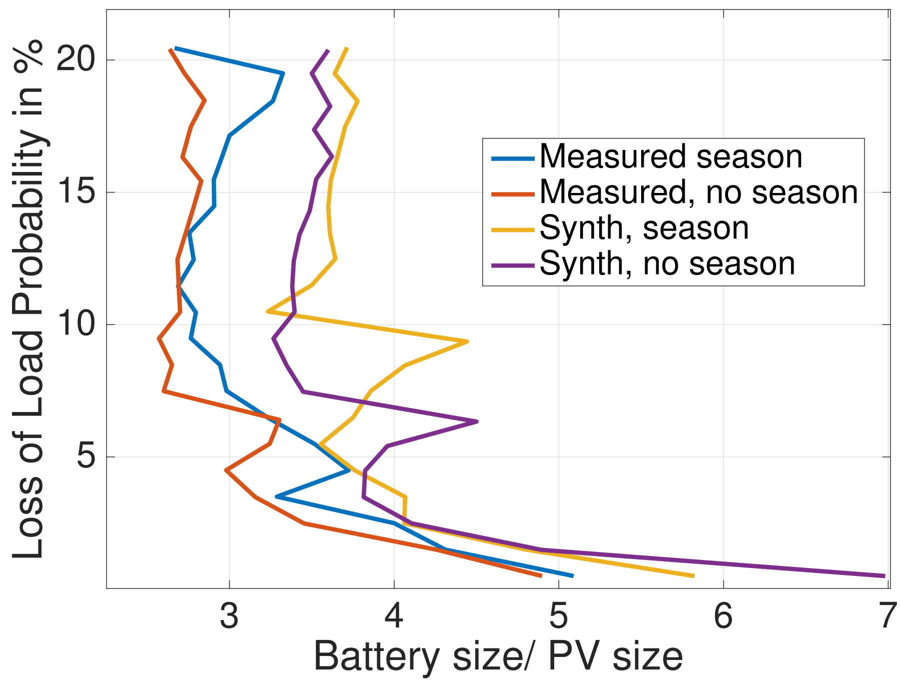

(b) The Battery/PV-size relationship to Loss of Load Probability

Figure 6.4: Graphical representation of some results from the system optimization. System investment cost increases with increased reliability. It is also seen in (b) that reliability is bought through increasing the proportion of batteries in the system.

Table 6.2: Optimal system composition for different scenarios at different Loss of Load Probabilities. As all systems have the same annual energy, the systems with seasonal variation will have higher peak-load during summer, and lower during winter, compared with those with no seasonal variation. This is seen in the increased PV-size for systems with seasonal variation.

	Measured load-profile				Synthesized loadprofile			
LLP [%]	Seasonal var		No variation		Seasonal var		No variation	
	PV	Batt	PV	Batt	PV	Batt	PV	Batt
0.5	390	1985	295	1445	340	1980	280	1955
1.5	370	1595	270	1150	330	1585	285	1395
2.5	340	1360	265	915	325	1320	280	1150
3.5	330	1085	255	805	300	1220	270	1030
4.5	290	1080	245	730	290	1090	255	975
5.5	280	985	225	730	280	995	240	950
6.5	275	890	215	710	260	975	220	990
7.5	270	805	225	585	245	945	235	810
8.5	260	765	215	570	230	935	230	770
9.5	255	705	210	540	215	955	225	735
10.5	245	685	200	540	235	760	215	730
11.4	240	645	195	525	220	770	210	710
12.5	230	640	190	510	210	765	205	695
13.5	225	620	185	505	205	740	200	685
14.5	215	625	180	500	200	720	195	680
15.5	210	610	175	495	195	705	190	670
16.3	205	605	175	475	190	695	185	670
17.1	200	600	170	470	185	685	185	650
18.4	190	620	165	470	180	680	180	650
19.5	185	615	165	450	180	655	180	630
20.4	195	520	165	435	175	650	175	630

7 TIME DOMAIN MODEL OF OPTIMIZED MICROGRID

Having the optimized system from Chapter 6, it would be of interest to see how it performs both in the long run, and for short-time studies.

In this chapter, two models to accommodate for such studies will be presented. One yearly model, purely mathematical, showing the overproduction, energy delivered by the battery, and the lost load.

For more detailed load-flow analysis, a 24 hour model has been developed by Quinard [40], much based on the works of Eleder [15]. This 24 hour model is made in Simulink, and utilizes inbuilt Simulink-blocks.

7.1 LONG TERM - YEARLY SIMULATION

This yearly simulation is an extension of the optimization model made by Mandelli [28]. It uses the same input-values as irradiation, ambient temperature, and a load-profile, in addition to the optimal size of the system, PV-panels in kW and battery-pack in kWh. As a simple mathematical model, it is just evaluating production, consumption and available energy in the battery at each time-step (per hour in this case). Production, consumption, and the needed power from the battery is saved in arrays for every time-step, as well as the Lost Load (when there is no production or sufficient power in the battery) and overproduction (full battery, and a surplus of electricity from the PV-panels).

The model considered losses in the inverter and the DC/DC-converter to the battery. Losses were given as converter-efficiencies, with a 90 % efficiency for the inverter, 85 % efficiency when charging the battery, and 90 % efficiency for discharge of the battery. Regarding the battery, this is simply modelled as a pool and internal losses or structures of the battery are not in any way considered.

It must be emphasised that this full-year load flow model is very simplified, and is to give an idea on when the power-shortage appears, and also if there is a lot of surplus energy produced by the system.

In order to simply compare different system, the battery State of Charge (SoC) was used as unit for the energy present in the system. The SoC is a number on how much energy there is in the battery, as a fraction of battery capacity. SoC of the battery is calculated as follows:

$$\mathrm{SoC} = \frac{E_{batt,current}}{E_{batt,max}} \tag{7.1}$$

and is unit-less. Plotting the battery SoC together with excesses production and Loss of Load per hour, results in Figure 7.1b.

As explained in Duus et al. [13], the solar and water resources in Bhutan complete each other very well. When there's excess of one, there's scarcity of the other. This would work well for combined systems with hydro and PV. Investigating Figure 7.1b together with Figure 7.1a shows it is during the monsoon that the power shortage occurs. Not strange as this is when the solar resources are at their lowest, and consumption is at it's peak (see Figure 3.5).

The green section of Figure 7.1b show over-production, energy which is not utilized by the system, as the load is served, and the battery is full. In case of grid-connection, this excess energy can be sold, reducing the payback time of the system. During the summer-months the consumption is the highest, and the solar irradiation is at its minimum (due to the monsoon). This makes for an unfortunate coincidence, and will be dimensioning for the system, which then for other times of the year could be considered over-dimensioned.

7.2 TIME DOMAIN RESPONSES FROM MEASURED CASE

To investigate better how the system behaves on a shorter time-scale, a 24 hour model was created. This is a complete model of a microgrid including the power sources, their power electronics, a load and mains model using MatLab and Simulink. The model is based on the works of Eleder [15], Mohamed [29], which was then edited and remastered by Quinard [40] during an internship at NTNU summer 2015.

This is a steady-state analysis, and also used to investigate changes in load, which occur over the day. One second in the model is representing one hour, giving the model a run-time of 24 seconds.

7.2.1 *System model components and composition*

The layout of the system for the 24 hour simulation is presented in Figure 7.2, clearly consisting of PV-panels, batteries and a load, along with converters and inverters.

In the following, the different components in the model will be explained.

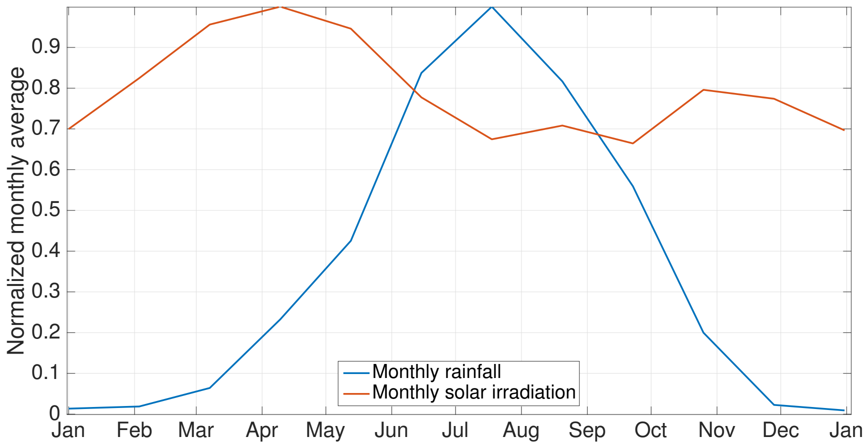

(a) Annual rainfall and irradiation

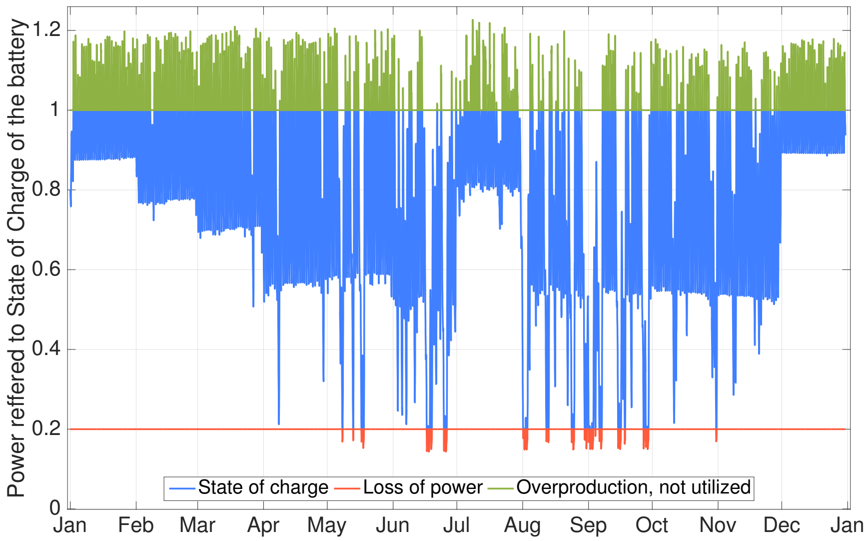

(b) Battery SoC over the year

Figure 7.1: Average monthly irradiation and rainfall is plotted together, to show negative correlation. During the monsoon (June-August) there is a lot of rain, and less sun. This clearly impacts power-production, seeing it's these months the LLP occurs (red). The green area is overproduction which is not stored in the battery and must be disposed of. Power in the battery is referred to State of Charge, 1 being full, and 0 being depleted. Simulation here is run with a minimum allowed SoC of 0.2.

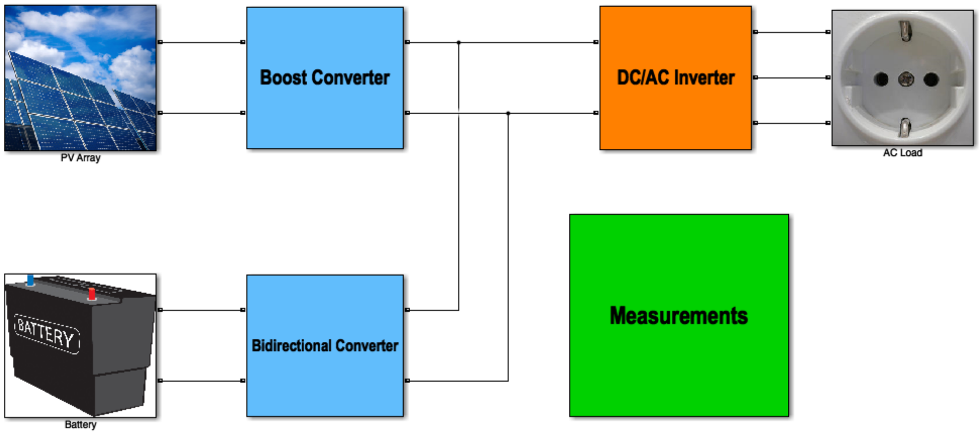

Figure 7.2: System layout for the 24h model. The system is composed of different blocks, each representing different parts of the system.

7.2.1.1 *PV-panels*

The production unit in this microgrid is the PV-panels. The model taking the input of optimal size, along with irradiance- and temperature-data, and simulates the output current and voltage.

The calculation of output power from the PV-panel in question is done mathematically, based on a number of equations from Eicker [14] and Eleder [15]. The equations which are utilized are based only on parameters that are given by the manufacturer for a typical cell, listed in Table 7.1.

Calculation of the photon-current at current operating cell-temperature:

$$I_{ph} = I_{ph,STC} + a_I \times (T_{cell} - T_{ref}) \tag{7.2}$$

$$I_{ph,STC} = I_{sc} \times \frac{Irr}{Irr_{stc}} \tag{7.3}$$

Calculation of diode saturation current:

$$I_0 = I_{ph} \times \exp \frac{\frac{-qV_{oc}}{n_s}}{nkT_{ref}} \tag{7.4}$$

T_{cell}	Cell temperature calculated from ambient temperature
Irr	Solar irradiance in W/m^2
Irr_{stc}	Solar irradiance at standard test conditions = 1000 W/m^2

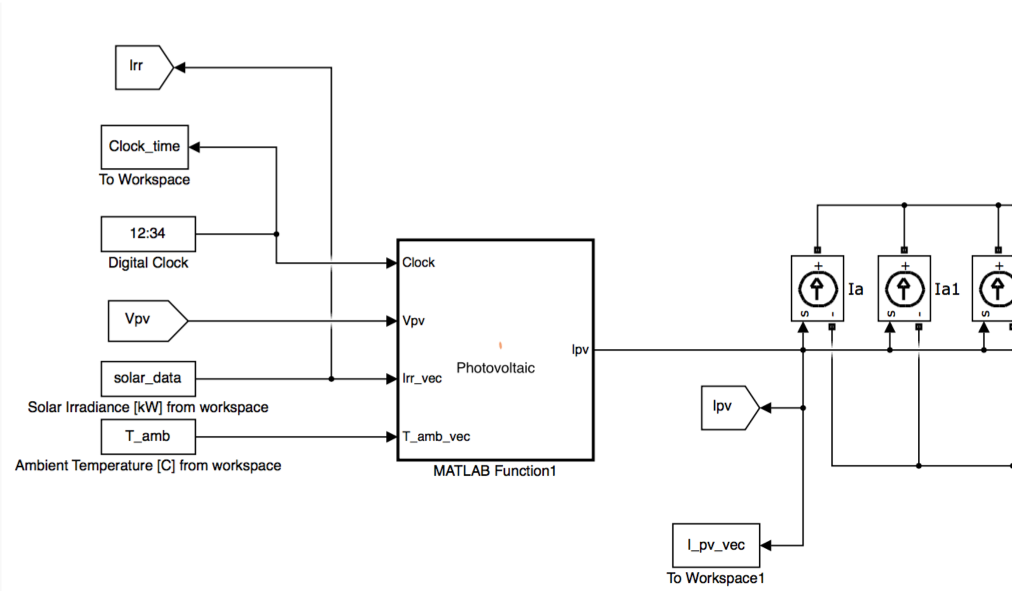

Figure 7.3: PV-array in 24hour model. The different input-variables to the Matlab-function are clearly visible on the left. This is used to calculated a PV-current, which is then run in to a series of diodes, simulating the behaviour of a real PV-panel. This gives a voltage output, and thus output-power can be calculated.

Table 7.1: Module specifications typically given by the manufacturer.

V_{oc}	Open circuit voltage per module $[V]$
I_{sc}	Short circuit current per module $[I]$
V_{MPP}	Voltage at maximum power point (MMPT) $[V]$
I_{MMP}	Current at MPPT $[I]$
P_{mod}	Maximum power per module (equals $V_{MPP} \times I_{MPP}$ $[W]$)
a_V	Decrease in voltage per °C increased from STC [p.u.]
a_I	Increase in current per °C increased from STC [p.u.]
P_{syst}	System size $[W]$
n_s	Number of cells in a module (typically 36 according to [36])

Table 7.2: Constants used for calculating the PV-current.

$k = 1.38e^{-23}$	Boltzmann's constant
$q = 1.60e^{-19}$	Electron charge
$n = 2$	Diode quality factor
$V_g = 1.12$	Band-gap voltage (1.12 for xtal Si, 1.75 for amorphous Si [15])
$T_{ref} = 25$	Nominal ambient test-temperature for panels at STC [°C]
$T_{nom} = 47$	Nominal operating cell-temperature [°C]

Calculation of the series resistance:

$$R_s = \beta \times \log\left(1 - \frac{I_{MPP}}{I_{ph}}\right) + \frac{V_{oc} - V_{MPP}}{I_{MPP}} \tag{7.5}$$

Where:

$$\beta = \frac{q}{n_s \times n \times k \times T_{cell}}$$

Calculation of PV-array current:

$$I_{pv} = I_{ph} - I_0 \times (\exp(\beta \times (V_c + I_{pv} + R_s) - 1)) \tag{7.6}$$

$$V_c = V_{pv}/NS$$

Seeing that the calculation of I_{pv} in Equation 7.6 is a differential equation, five iterations of Newton-Rhapson method is used to solve this. V_{pv} is the measured output-voltage from the PV-panels.

Newton-Rhapson:

$$I_{pv,2} = I_{pv,1} - \frac{f(I_{pv,1})}{f'(I_{pv,1})}$$

7.2.1.2 *Battery-storage*

The battery-storge in this case is modelled very simply with the internal battery-block from Simulink, connected on the DC-bus.

Over the course of mentioned summer-internship, a lot of work was done to properly include a Buck-Boost-converter for the battery, while maintaining

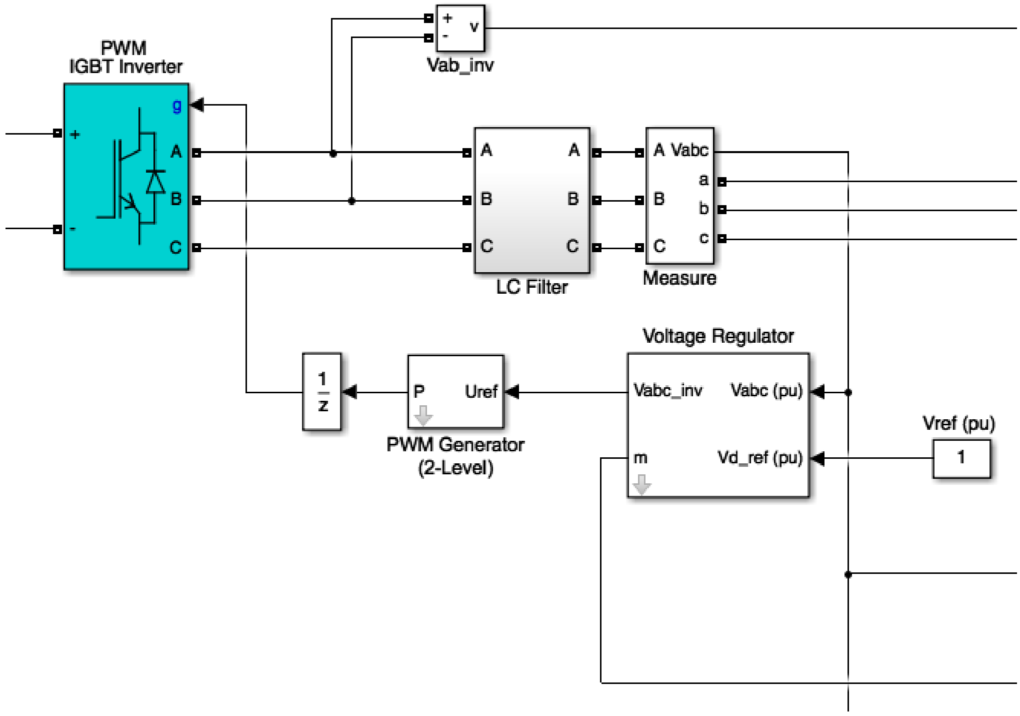

Figure 7.4: Topology for the inverter-controls.

a reasonable low simulation-time. This work proved to be unsuccessful, and thus a simplified solution was chosen.

The charge-controller is designed to use the battery to stabilize the voltage on the DC-bus, charging and discharging in order to keep the voltage constant.

7.2.1.3 *Inverter and load*

To convert the current from DC to AC, a three-level IGBT/Diode inverter is used, this is a regular matlab/simulink-block. A simple voltage control loop is being utilized, as displayed in Figure 7.4.

There is also a block which includes filters, to reduce the amount of harmonics in the output AC-current. As of now, the Bhutanese grid-codes, found in Bhutan Electricity Authority [6] do not regulate harmonics specifically, and thus the Norwegian gird-codes in Olje- og energidepartementet [32] will be used in this regard.

The load was simply modelled as a step-function, with a base-load of 40 kW active power and 500 VAr, and adding a 10 kW to this between 18:00 and 23:00. This simple modelling of the load was done due to numerous errors and prob-

Table 7.3: Norwegian crid code regulations for harmonics in the system. Collected from Lovdata 07.10.2015. Total harmonic distortion shall never exceed 8 % and 5 % measured over a period of 10 minutes and one week respectively.

Odd harmonics				Even harmonics	
Non-multiple of 3		Multiple of 3			
Order h	U_h	Order h	U_h	Order h	U_h
5	6.0 %	3	5.0 %	2	2.0 %
7	5.0 %	9	1.5 %	4	1.0 %
11	3.5 %	> 9	0.5 %	> 4	0.5 %
13	3.0 %				
17	2.0 %				
19, 23, 25	1.5 %				
>25	1.0 %				

lems implementing a dynamic load in the model. This must be implemented later on, when further developing the model.

7.2.2 *Results*

This short-term time-domain simulation can be used for detailed studies of the system. At this stage, the presented model is not fully functioning, with all the desired functions and flexibility, however some initial results can be presented.

Possible future implementations could be options for short-circuit analysis, alternate control-loops, or investigating system behaviour in the case of battery-depletion and no power from the PV-panels.

7.2.2.1 *Voltage and harmonic distortion*

As mentioned, there are currently no grid-codes in Bhutan to limit the amount of harmonics in the system, thus the Norwegian grid-codes were utilized fort his purpose.

Without any kind of filtering, the amount of harmonics was well exceeding acceptable values displayed in Table 7.3. Thus three passive filters were installed to reduce the noise to be within given values. The filters used were the already-existing Simulink-blocks, tuned to the maximum load.

The results with filtering can be seen in Figure 7.5, and with the resulting FFT-analysis executed with the inbuilt functions in Simulink in Figure 7.6. It

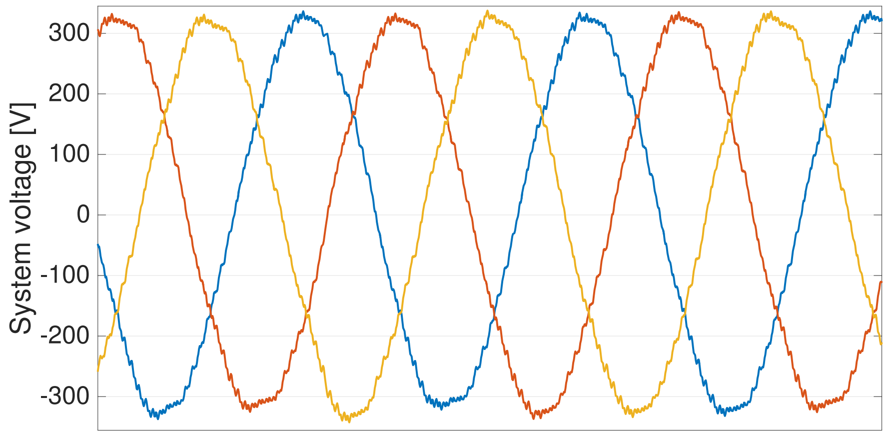

Figure 7.5: Phase-voltages in the system. Harmonic distortion is visible on all phases to some extent.

is here seen that the thresholds presented in Table 7.3 are not exceeded. The filters installed have thus done their job in reducing the harmonics.

However, further work with the model, with better control-loops can make it able to run without filters, and still not violate set regulations.

Investigating Figure 7.5 shows a symmetric three-phase system, as is to be expected, but the harmonic distortion is still visible, especially at the peaks.

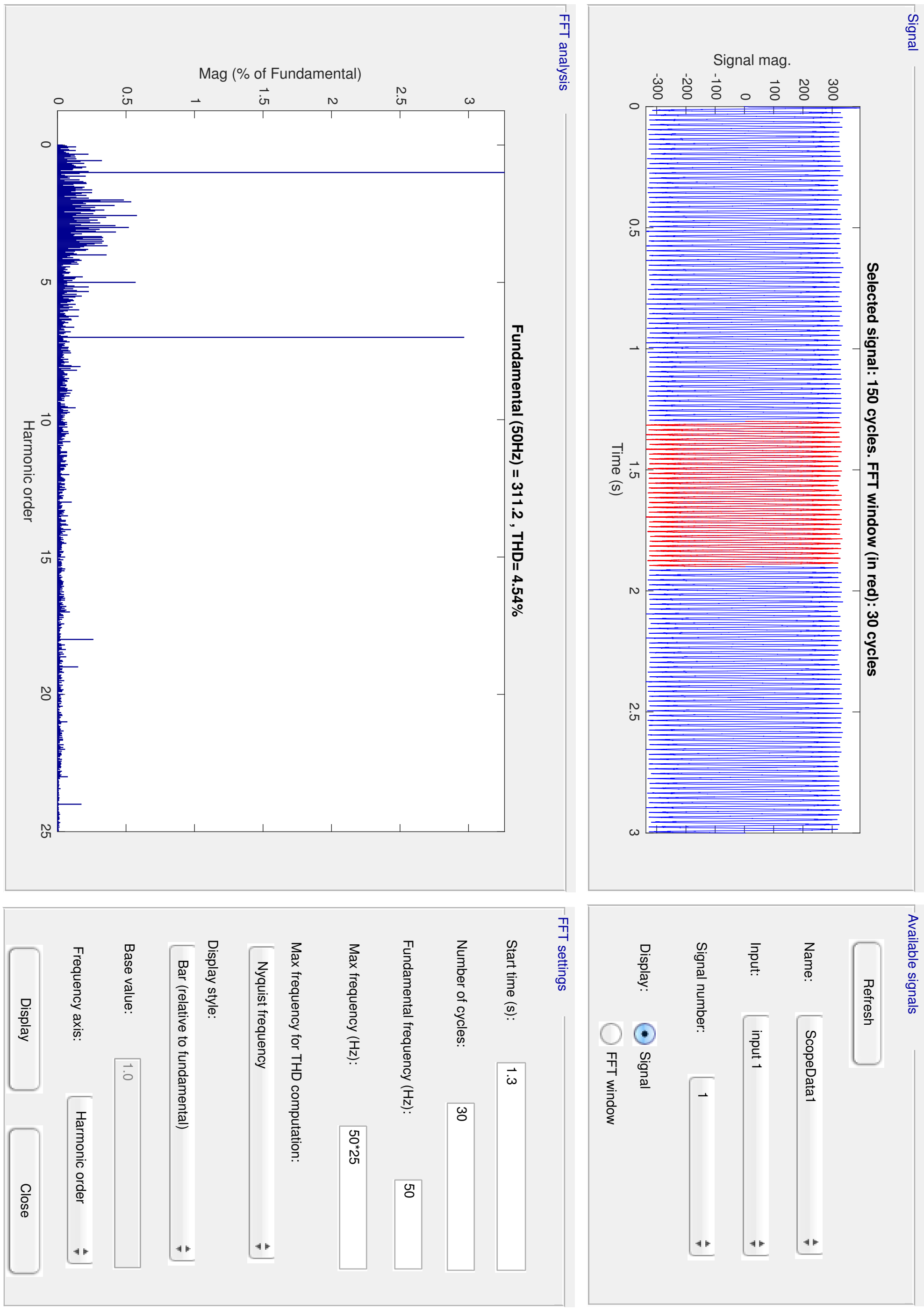

Figure 7.6: FFT analysis for the 24 hour simulation executed in Simulink. It is evident that the limits for harmonics are not exceeded.

8 CONCLUSIONS AND FURTHER WORK

The goal of this thesis was to present a full-path methodology for dimensioning and assessing islanded microgrids in rural areas. Everything from data acquisition to operating system and a dynamic model has been presented, along with the advantage of the novel sizing methodology over other already-existing tools. There is still some work needed to fully complete and make operative software, but it is a first building-block towards a novel sizing methodology, which cover all these aspects, and can be used freely by everyone, everywhere.

The methodology presented has been applied to a real case in Bhutan, where the measured consumption-data has been compared to those done on basic assumptions. The resulting systems did not differ much in the two cases, thus confirming that it is indeed possible to do preliminary assumptions based on simple data, but still getting a result close to reality. These are important observations, as the data basis for dimensioning microgrids in rural areas often can be scarce.

Another observation done in the work of the thesis, is the relative change in system-composition at low LLPs, depicted in Figure 6.4b. This change in system-composition can be used as argument for designing islanded microgrids with higher LLP to get most PV-panels from the budget and maintaining optimal composition. It could further be the basis for a future framework for setting dimensioning LLP for a system, a framework which, to the best of the authors' knowledge, does not yet exist.

Further work would mainly consist of improving the time domain model, for more flexibility and stability. The overall model also needs a simple user interface, enabling those without intimate programming-knowledge to utilize the methodology and make decisions based on its outputs.

Simpler ways of giving input-data to the system would be desired, along with a complete program, doing all the operations in one go. As of now, each step must be done separately, which would be inconvenient for an end-user.

Also real testing on a full scale system with an optimized composition of PV and batteries is of great interest, in order to evaluate whether estimated parameters such as power production and LLP would coincide with measured values. Studies like this would be an important step in affirming that the methodology indeed works as it should, and provides the user with optimal solutions.

A APPLICATIONS TO OTHER SYSTEMS

During the literature-study for this thesis, a study by Tonny [50] was discovered. It is investigating PV/battery-systems for domestic use in Bangladesh, and provides almost all the information needed to conduct the system-optimization based on the methodology presented in this paper.

As a curiosity, it was decided to indeed try and optimize one of the systems presented to see whether it was most optimal for the consumer.

Here follows a short description of the process, along with the results.

A.1 BANGLADESH

Bangladesh is considered a lower-middle-income country by The World Bank [49], and has difficulties to build conventional electric infrastructure due to the topography of the country. As of 2008 there was a 800 MW deficit in power-production compared to consumption, and power-shortage is still very present in the country. Small PV installations can play a key-role in closing this energy-gap.

This is investigated in Tonny [50], where the Bangladesh Rehabilitation Assistance Committee (BRAC) Solar Energy Program, initiated in 1998, is being analysed. The survey in the study is done to understand the progress BRAC takes towards rural electrification through solar energy, with an aim to analyse social impact, and also contribute technically to improve the performance of solar home systems (SHS).

In Table 4.2 in Tonny [50] one can see the different systems, with appliances, what it can deliver, and for what price. It operates 4 hrs/day, typically in the evening when there is a need for lightning indoors.

He further lists the alternatives which are used to electricity, being candles, kerosene lamps, and a charged car-battery to supply a TV with electricity. The car-battery needs to be recharged 2 times / month. From these details the value of lost load can be calculated (this is also done in [50]).

Tables 4.5 and 4.6 (reproduced in Table A.1 and Table A.1) in [50] are very similar in information to Table 3.3, which is what is required to make a synthesized load-profile for optimizing a system utilizing the novel optimization methodology explained in this thesis.

Table A.1: Overview of appliance operating hours over a day in a household in Bangladesh, reprinted from table 4.5 in Tonny [50]

ACTIVITY	MORNING	AFTERNOON	EVENING	NIGHT
Light			18:00-19:00	19:00-22:00
Radio	07:00-08:00			
TV			15:30-19:00	19:00-21:00

Table A.2: Overview of appliances and respective energy consumption per day in a household in Bangladesh, reprinted from table 4.6 in Tonny [50]

APPLIANCES	$P[W]$	USE $[h/day]$	E/DAY $[Wh]$
Lamp 1 (reading)	6	5	30
Lamp 2 (bedroom)	6	4	24
Lamp 3 (bedroom)	6	2	12
Radio	10	1	10
TV (black & white)	20	4	80
SUM			**156**

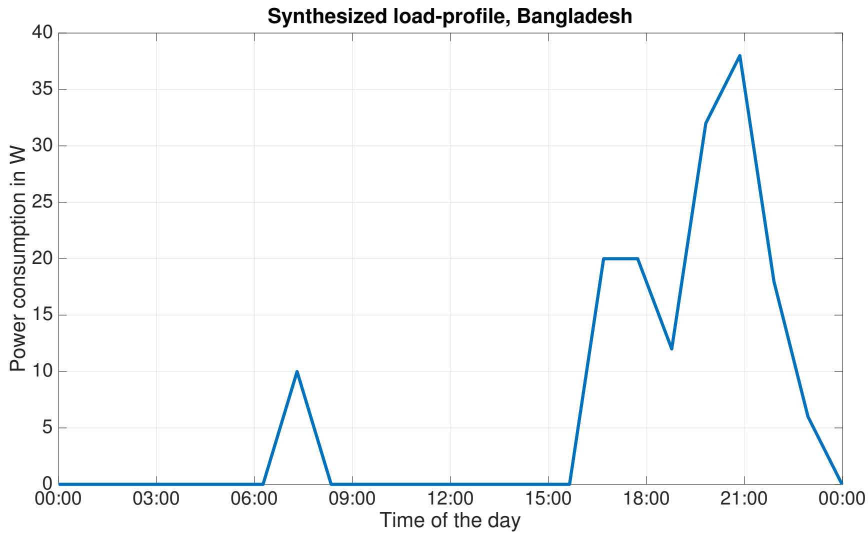

Figure A.1: Based on the data given in Table A.1 and Table A.1, this becomes the synthesized load-profile. The methodology used to produce the load-profile is with excel, explained in Section 3.1.2

For the optimization process the following assumptions were made:

- Customers seem overall satisfied with the system, which would imply a low degree of outages while operating. Assuming a loss of load to $< 2\%$.
- The information given in Table A.1 and Table A.2 are correct, and operating-windows are fully utilized.
- The batteries operate at a voltage of 12 V
- The deep discharge batteries used can tolerate a minimum SoC of 20 %.

According to table 4.2 in Tonny [50] an installation of 50 W with a battery of 80 Ah should be sufficient for the described system.

Using this data to create a load-profile, and also acquiring solar-data from NASA for the site, the optimal size for the system was found.

Without going into the details, our findings were that the optimal composition of the system would be about 90 Wp of PV, and 370 Wh of batteries (current battery-pack is 80 Ah * 12V = 960 Wh). The reduction in battery-size is quite significant, with a reduced size by more than 60 %. Even with the increase in PV-size, the total system cost will most likely go down, and with a reduced cost, more families may afford an SHS.

This is just a simple example showing that taking time to optimize a system according to user needs will pay off in the long run.

B

MEASURED CONSUMPTION FROM CST

Here follows information on power-consumption measurements done at the College of Science and Technology (CST) during the field-trip in September-October 2015. An elaboration on how the measured load-profile used for the calculations in Chapter 6 was made is also presented.

Finally some thoughts on the initial assumptions, and how they compare with the real case, will be given.

B.1 MEASUREMENT EQUIPMENT AND SET-UP

In order to check the validity of the synthesized load presented in Figure 3.3, measurement-devices was installed at CST. The Norwegian University of Technology and Science (NTNU) provided simple smart-meters that log power-consumption every minute, for a period of 30 days, before the data must be collected. The smart-meters is produced by OWL®, and documentation is found at The Owl [48].

At CST each floor in the student-residents were fed by a single-phase power-line. This was very convenient as the OWL-meters only measure on one-phase cables, and thus no changes in the original electrical set-up had to be done in order to do the measurements. A picture of the system set-up is presented in Figure B.2. The clamps on the cables are clearly visible, and each clamp is connected to a logger, which then wirelessly sends the data to the small computer, which both displays and stores the information for the next 30 days. Real-time power consumption can be glimpsed on the display in the figure.

The measurements was be done on each of the three phases at the power intake for buildings A, E, RK and Library. A total of 12 measurement devices was used, three for each phase in each building. They would measure the current passing through the cable with a farad-coil, and the power would then be calculated using the measured current, and a preset voltage. Grid-voltage in Bhutan is 230 V, so this value was preset on all devices before measuring started.

To verify the voltage indeed being 230 V, a voltmeter with logger was installed at the library-building, measuring voltage every minute from 25.09.15 09:39 hr to 26.09.15. 22:54 hr. The average voltage over the period was 225.6 V, and is depicted in Figure B.1. According to Table 5.4.2 in Bhutan Electricity Authority [6], the limits of variation in the low-voltage grid is ±6%. These limits

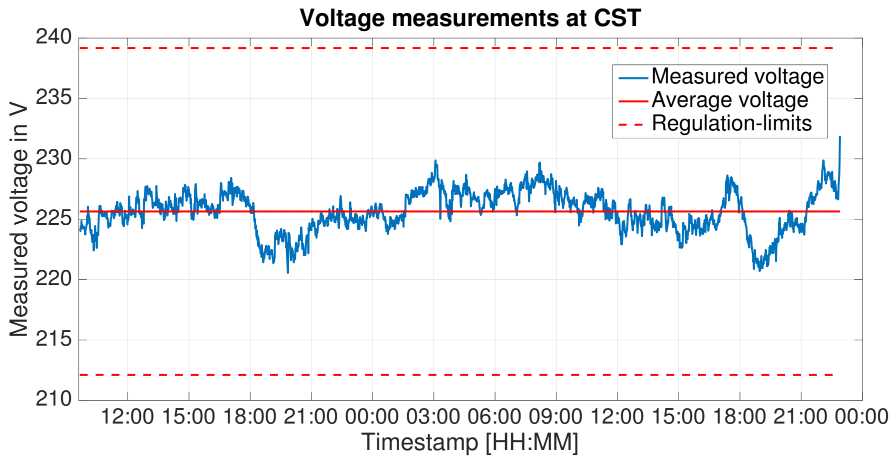

Figure B.1: Measured voltage with one minute intervals at CST from 25.09 to 26.09. It is clear that the voltage is within the regulation boundaries (doted red) at $\pm 6\,\%$

are shown in Figure B.1 as doted red, and it is clear that the measured values are well within these limits.

Naturally the voltage-drops at 18:00 h coincide with the increased consumption at this hour, clearly depicted in Figure B.3. This also relates to the time of sunset, which in a way marks the end of the day outside, and force the students inside, and to use power for lightning and fans in their rooms.

B.2 RESULTS - ENERGY CONSUMPTION

Measuring power consumption in different buildings for more than two weeks, resulted in a lot of data. However, two of the installed twelve meters was dysfunctional, and had not properly logged data for the period. These two meters has thus been neglected from further studies, resulting in only two measurement devices for Block RK and Block A.

The resulting consumption for Block E is depicted in Figure B.3. Daily variations are evident, with most of the consumption happening during the evening. Also worth noting is the unbalance in the system between the phases, as each floor only has a one phase cable the connected load per phase will vary to a greater extent than what might be expected.

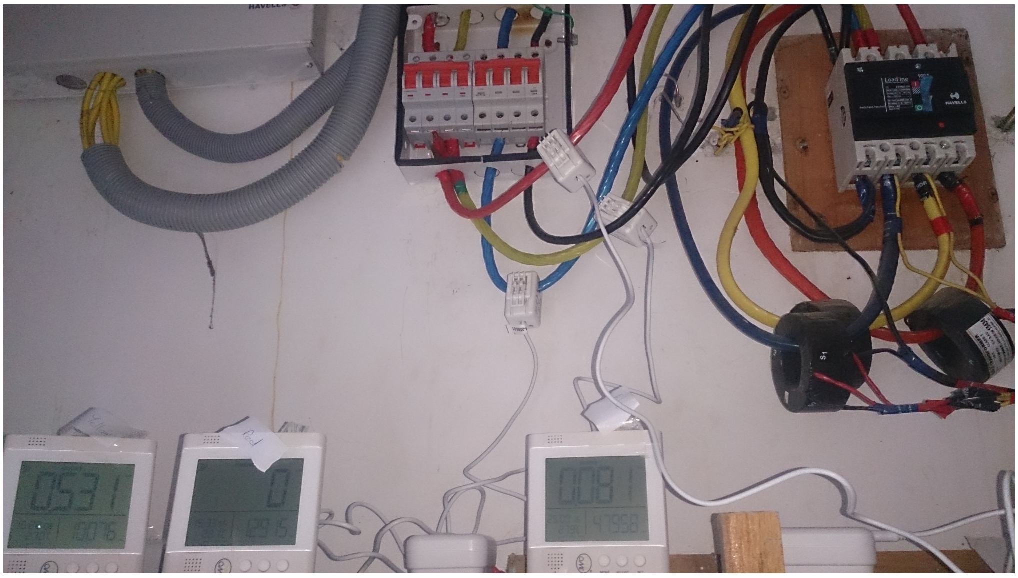

Figure B.2: The measurement devices were each connected to a one phase cable, and measured the passing current using a ferrite-coil. Each coil had it's own meter, showing real-time power consumption for the given phase.

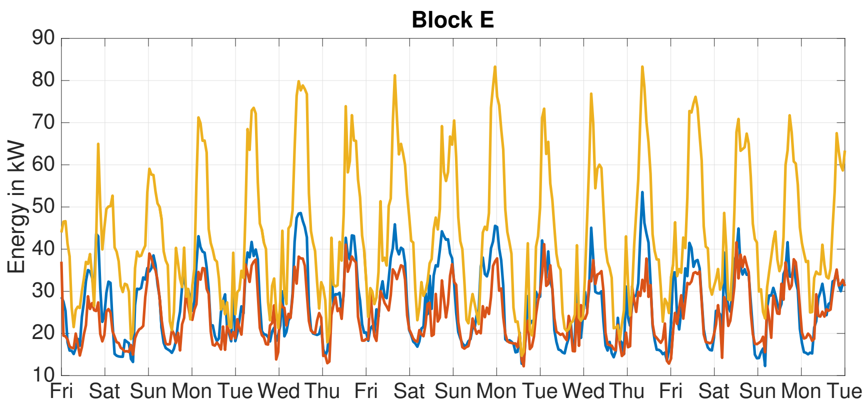

Figure B.3: Power consumption measured in Block E in the period of 25.09.2015 to 12.10.2015. Little change is observed between week-day and week-end, and it is clear that the peak-power occurs after sunset. Vertical grid-lines are at 00:00 hr (midnight)

Creating a load-profile

In the following, measured consumption data from the CST will be presented, along with the methodology employed in order to create the daily load-profile used for the calculations in Chapter 6.

After the field-trip in Bhutan, the authors had 16 full days worth of measurements from Block-A, Block-E, Block-RK and the library-building, measured on all three phases. Some of the measurements proved to be corrupted and thus invalid, leaving only measurements on two phases in Block-A and Block-RK. The library-building will be excluded from the analysis, at it has a different behavioural pattern than the hostel-blocks, much lower energy-consumption, and does not house students.

In order to get the best fit of a "normal" day, all the measurements for each phase was split up into separate days, giving 16 "days" per block per phase, resulting in 112 individual days measured. These values were then averaged, giving a load-profile which represents an average phase in an average hostel-block. All the data for each individual day is plotted in Figure B.4, both for the original one minute resolution, and also for a one hour average.

The initial measurements on consumption were done on a minute-basis, but the general time-step of the calculations done in the thesis is in hourly resolution, thus the final profile was given with hourly resolution. Both profiles are depicted in Figure B.5.

B.3 EVALUATION OF INITIAL ASSUMPTIONS COMPARED TO REAL CASE

Many of the base-assumptions for the synthesized profile used in Chapter 6 was done without much real knowledge to the local conditions in Bhutan. Only some information was given by the students and staff at the CST, which then was used for the analysis. Looking at Figure 6.2 reveals a distinct difference between the actual consumption, and the synthesized load.

The synthesized load has a much higher night-peak, and next to no base-load. If this really was the case should have been checked, simply by asking whether or not the students would be in their rooms at all during daytime. Another way of getting this information could've been to ask a few students to describe a typical day in a paragraph or two. This would give a better context to the technical information provided.

Another thing which should have been considered to a greater extent is the impact daylight has on everyday-life.

However, looking at the resulting optimized system for the two cases, they are not all that different, as discussed in earlier chapters. This gives credibility to the bottom-up approach on building load-profiles, starting with the appli-

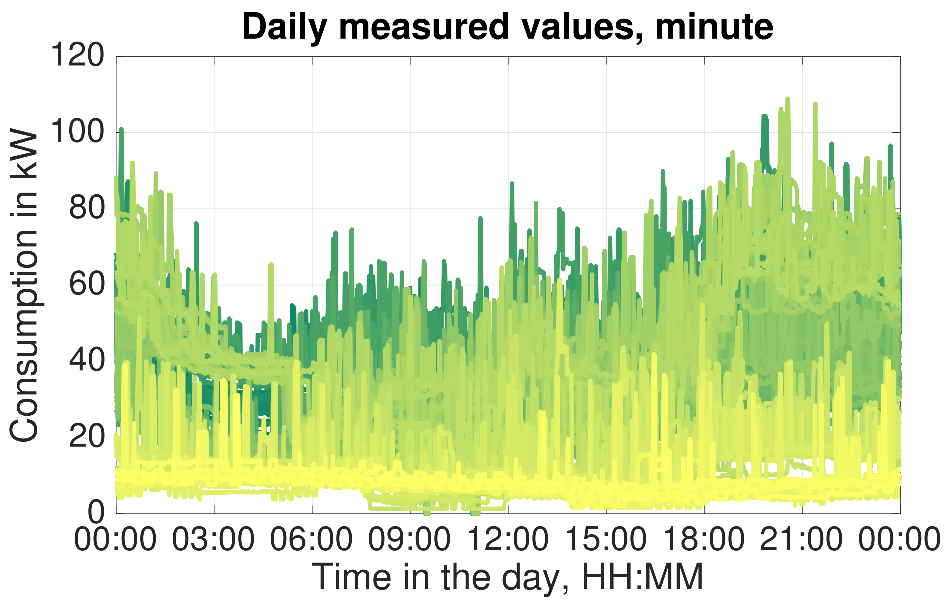

(a) Mesurements every minute

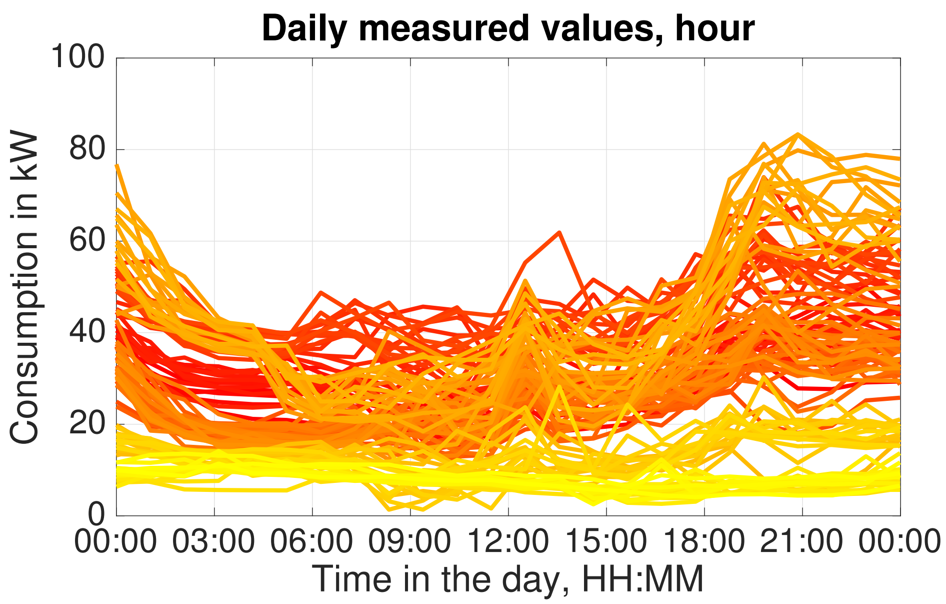

(b) Measurements every hour

Figure B.4: These are the measured values of power-consumption at the CST, each line represents one phase. It is seen that some of the peaks that occur in Figure B.4a are gone in Figure B.4b due to the averaging over the time-period.

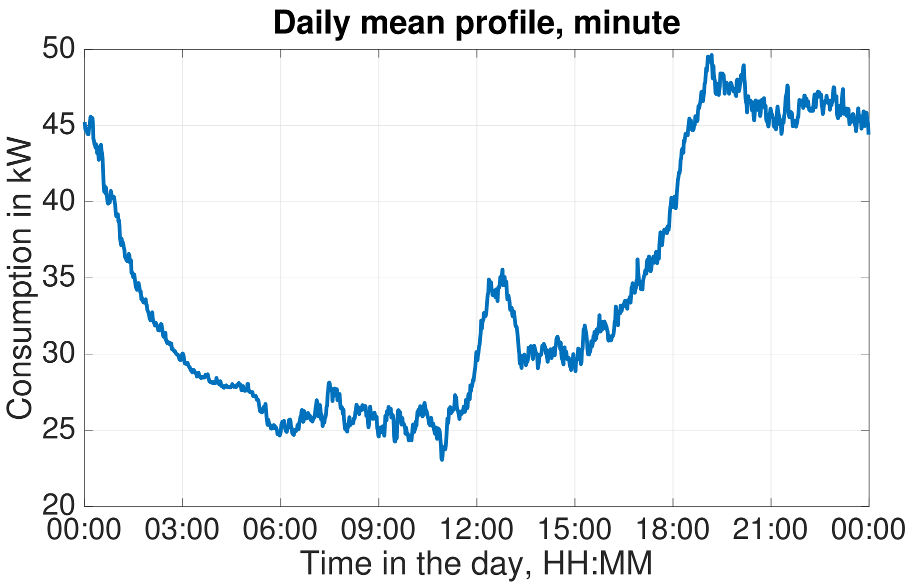

(a) Averaged daily profile, minute resolution

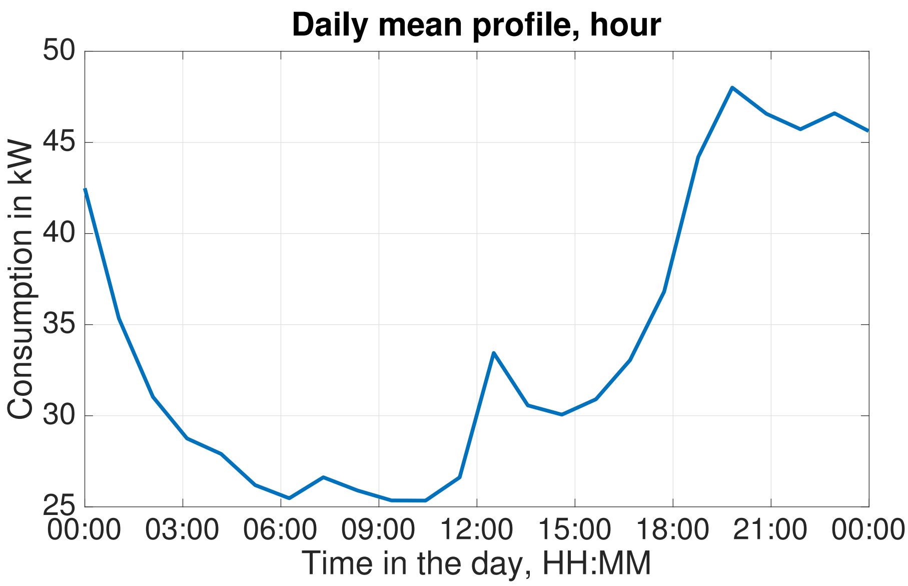

(b) Averaged daily profile, hourly resolution

Figure B.5: Using the measured data acquired at the CST to create an averaged consumption-profile, depicted with both resolution of one minute and one hour.

Table B.1: Measured power-consumption per block at the CST campus. All values are in kWh, and the measurements go from April 2014 to August 2015. Meters were installed halfway into April 2014, resulting in lower metered consumption this month than what is to be expected.

	Mess	Block-E	Block-D	Block-C	Block-A	Block-B	Hostel LH	Hostel RH	SUM
Apr	329	1560	1560	1240	1480	1240	960	1120	9489
May	222	3400	3160	2600	3200	2600	2480	2480	20142
Jun	270	4120	3760	2800	3680	3000	2800	2920	23350
Jul	63	1680	2040	1000	1760	920	920	1240	9623
Aug	344	3880	3160	2440	3400	2480	2760	2840	21304
Sep	304	3400	3120	2640	3280	2440	2800	2840	20824
Oct	350	3560	2960	2760	3160	1720	2680	2640	19830
Nov	233	3560	2800	2880	2800	2000	2640	2720	19633
Dec	91	1880	0	0	0	0	1360	1240	4571
Jan	3	1760	120	920	480	40	600	1280	5203
Feb	77	2080	1160	1080	1680	560	1680	1720	10037
Mar	55	2200	2080	2040	2120	1240	1960	1960	13655
Apr	121	3200	2960	2840	3040	2280	2640	3400	20481
May	173	2760	2640	2320	2680	2040	2320	3080	18013
Jun	230	3200	3160	2800	3280	2520	2840	3720	21750
Jul	72	920	1360	880	1920	1080	1120	2080	9432
Aug	428	4160	3680	3080	3880	3240	3320	4400	26188

ances connected to the system. Such an approach is also understandable for the end-user, which has an idea on how their consumption is over the course of a day.

In conclusion, get as much data as possible from the locals, and also understanding their every-day-life is key to making the best approximations. This is of course best done by visiting and living at the site, giving invaluable insight and information in the process.

BIBLIOGRAPHY

[1] Camilla Aabakken, Hege Sveaas Fadum, Astrid Anestad, Fredrik Hageengen, and Ragnhild Aker Nordeng. Avbrotsstatistikk 2013. Technical report, Norges Vassdrags- og Energidirektorat, 2014.

[2] Abdirahman Mohamed Abdilahi, Abdul Halim Mohd Yatim, Mohd Wazir Mustafa, Omar Tahseen Khalaf, Alshammari Fahad Shumran, and Faizah Mohamed Nor. Feasibility study of renewable energy-based microgrid system in Somaliland's urban centers. *Renewable and Sustainable Energy Reviews*, 40:1048–1059, 2014. ISSN 13640321. doi: 10.1016/j.rser.2014.07.150. URL http://linkinghub.elsevier.com/retrieve/pii/S1364032114006029.

[3] Atmospheric Science Data Center. Surface meteorology and Solar Energy. https://eosweb.larc.nasa.gov/sse/. Accessed: 2015-06-18.

[4] Australian Space Academy. Orbital Parameters, Low Earth Orbit. http://www.spaceacademy.net.au/watch/track/leopars.htm. Accessed: 2015-09-02.

[5] Subhes C. Bhattacharyya. Review of alternative methodologies for analysing off-grid electricity supply. *Renewable and Sustainable Energy Reviews*, 16(1):677–694, 2012. ISSN 13640321. doi: 10.1016/j.rser.2011.08.033. URL http://dx.doi.org/10.1016/j.rser.2011.08.033.

[6] Bhutan Electricity Authority. Distribution Code. 2008.

[7] BlueSol. Photovoltaic design software. http://www.bluesolpv.com/dnnsite/default.aspx. Accessed: 2015-17-07.

[8] A. N. Celik. Effect of different load profiles on the loss-of-load probability of stand-alone photovoltaic systems. *Renewable Energy*, 32(12):2096–2115, 2007. ISSN 09601481. doi: 10.1016/j.renene.2006.11.002.

[9] D. Connolly, H. Lund, B. V. Mathiesen, and M. Leahy. A review of computer tools for analysing the integration of renewable energy into various energy systems. *Applied Energy*, 87(4):1059–1082, 2010. ISSN 03062619. doi: 10.1016/j.apenergy.2009.09.026. URL http://dx.doi.org/10.1016/j.apenergy.2009.09.026.

[10] Council of European Energy Regulators (CEER). CEER Benchmarking Report 5 . 1 on the Continuity of Electricity Supply Data update. (February): 1–23, 2014.

[11] Yangchen Dolkar, Dawa Jamtsho, Tshewang Lhendup, and Pema Lhamo. System Design and Performance Analysis of a Grid- Tied Solar PV Power System in Bhutan. In *IEEE International Conference on Computational Intelligence & Communication Technology*, pages 538–542, 2015. ISBN 9781479960231. doi: 10.1109/CICT.2015.55.

[12] Swapnil Dubey, G. S. Sandhu, and G. N. Tiwari. Analytical expression for electrical efficiency of PV/T hybrid air collector. *Applied Energy*, 86(5): 697–705, 2009. ISSN 03062619. doi: 10.1016/j.apenergy.2008.09.003. URL http://dx.doi.org/10.1016/j.apenergy.2008.09.003.

[13] Hakon Duus, Stefano Mandelli, Marta Molinas, and Olav Bjarte Fosso. A methodology for supporting the planning of microgrids based on composable tools: A case in Bhutan. In *2015 5th International Youth Conference on Energy (IYCE)*, volume 2015, pages 1–6. IEEE, may 2015. ISBN 978-1-4673-7171-1. doi: 10.1109/IYCE.2015.7180749. URL http://ieeexplore.ieee.org/lpdocs/epic03/wrapper.htm?arnumber=7180749.

[14] Ursula Eicker. *Solar Technologies for Buildings*. Wiley, 2003.

[15] Araneta Estala Eleder. *A modular simulation platform for testing hybrid DC/AC future grid solutions for remote areas*. PhD thesis, Mondragon University Faculty of Engineering, 2013.

[16] European Network of Transmission System Operators for Electricity (ENTSOE). Consumption Data. https://www.entsoe.eu/data/data-portal/consumption/Pages/default.aspx. Accessed: 2015-08-16.

[17] European Organisation for the Exploitation of Meteorological Satellites. EUMETSAT. http://www.eumetsat.int/website/home/index.html. Accessed: 2015-11-02.

[18] Fraunhofer Institute of Solar Energy Systems ISE. Photovoltaics Report. Technical Report August, aug 2015. URL http://www.ise.fraunhofer.de/en/downloads-englisch/pdf-files-englisch/photovoltaics-report-slides.pdf.

[19] Paul Gilman, Shannon Cowlin, and Donna Heimiller. Potential for Development of Solar and Wind Resource in Bhutan. Technical report, National Renewable Energy Laboratory, sep 2009.

[20] HOMER Energy. Hybrid Optimization of Multiple Energy Resources. http://www.homerenergy.com/. Accessed: 2015-17-07.

[21] International Energy Agency (IEA). Energy Poverty. https://www.iea.org/topics/energypoverty/. Accessed: 2015-08-30.

[22] Ali Keyhani. *Design of Smart Power Grid Renewable Energy Systems*. Wiley, 2011. ISBN 978-0470-62761-7.

[23] Tamer Khatib, Azah Mohamed, and K. Sopian. A review of photovoltaic systems size optimization techniques. *Renewable and Sustainable Energy Reviews*, 22:454–465, 2013. ISSN 13640321. doi: 10.1016/j.rser.2013.02.023. URL http://dx.doi.org/10.1016/j.rser.2013.02.023.

[24] Jan Kleissl. *Solar Energy Forecasting and Resource Assessment*. Elsevier Inc, 1 edition, 2013. ISBN 978-0-12-397177-7. URL http://www.sciencedirect.com/science/book/9780123971777.

[25] Eirik Oksavik Lockertsen. *The Performance and Potential for PV systems at Northern Latitudes*. PhD thesis, Norwegian University of Science and Technology, 2015.

[26] P Loka, S Moola, S Reddy, A Skumanich, S Fulton, S C Siah, and P Mints. A Case Study for Micro-Grid PV : Rural Electrification In India. 95032(1): 3379–3382, 2013.

[27] Anne Lozé. Use of HOMER Software. Technical report, Norwegian University of Science and Technology, 2015.

[28] Stefano Mandelli. *Strategies for Access to Energy in Developing Countries: Methods and Models for Off-Grid Power System Design*. PhD thesis, Politecnico di Milano, 2014.

[29] Faisal Mohamed. *Microgrid Modelling and Simulation*. PhD thesis, 2006.

[30] Matthew Muller. Measuring and Modeling Nominal Operating Cell Temperature (NOCT) (Presentation). Technical report, National Renewable Energy Laboratory, 2010.

[31] NASA Earth Observatory. Three Classes of Orbit. http://earthobservatory.nasa.gov/Features/OrbitsCatalog/page2.php. Accessed: 2015-09-02.

[32] Olje- og energidepartementet. Leveringskvalitetsforskriften. https://lovdata.no/dokument/SF/forskrift/2004-11-30-1557, . Accessed: 2015-10-07.

[33] Olje- og energidepartementet. Forskrift om kontroll av nettvirksomhet, Â§9-2 . http://lovdata.no/forskrift/1999-03-11-302/Â\protect\T1\textsection9-2, . Accessed: 2015-11-06.

[34] Photovoltaic Software. Professional Photovoltaic Softwares. http://photovoltaic-software.com/professional.php. Accessed: 2015-07-17.

[35] Manfred Pöchacker, Tamer Khatib, and Wilfried Elmenreich. The Microgrid Simulation Tool RAPSim: Description and Case Study. In *IEEE Proceedings of ISGT Asia 2014*, pages 287–292, 2014. ISBN 9781479913008. doi: 10.1109/ISGT-Asia.2014.6873803. URL http://ieeexplore.ieee.org/xpls/abs{_}all.jsp?arnumber=6873803$\delimiter"026E30F$nhttps://mobile.aau.at/publications/poechacker-2014-The{_}Microgrid{_}Simulation{_}Tool{_}RAPSim.pdf.

[36] PV Education.org. Nominal Operating Cell Temperature. http://www.pveducation.org/pvcdrom/modules/module-circuit-design, . Accessed: 2015-11-03.

[37] PV Education.org. Nominal Operating Cell Temperature. http://www.pveducation.org/pvcdrom/modules/nominal-operating-cell-temperature, . Accessed: 2015-11-03.

[38] PVGis. Institute for Energy and Transport, Joint Research Centre. http://re.jrc.ec.europa.eu/pvgis/imaps/index.htm. Accessed: 2015-11-02.

[39] PVSyst. Photovoltaic Software. http://www.pvsyst.com/en/. Accessed: 2015-17-07.

[40] Honorat Quinard. Modelisation of a PV- Microgrid. Technical report, Norwegian University of Science and Technology, 2015.

[41] RETScreen International. RETScreen. http://www.retscreen.net/ang/home.php. Accessed: 2015-17-07.

[42] Danielle Sakepa. Analysis of different software for the sizing and optimization of a micro grid in Phuntsholing (Bhutan). Technical report, Norwegian University of Science and Technology, 2015.

[43] Ernst Friedrich Schumacher. *Small Is Beautiful: A Study of Economics As If People Mattered*. Blond & Briggs, 1973.

[44] Walter Short, Daniel J Packey, and Thomas Holt. A Manual for the Economic Evaluation of Energy Efficiency and Renewable Energy Technologies. (March):120, 1995. URL http://www.nrel.gov/docs/legosti/old/5173.pdf.

[45] Arbi Gharakhani Siraki and Pragasen Pillay. Comparison of PV System Design Software Packages for Urban applications. In *XII World Energy Congress*, page 12, 2010. URL http://www.indiaenergycongress.in/montreal/library/pdf/285.pdf.

[46] SolarGis. Solar and PV data. http://solargis.info/doc/solar-and-pv-data. Accessed: 2015-11-02.

[47] Joshua S Stein, Richard Perez, and Andrew Parkins. Validation of PV Performance Models Using Sattelite-Based Irradiance Measurements: A Case Study. In *ASES National Solar Conference 2010 Phoenix, AZ*, 2010.

[48] The Owl. Intelligent Wireless Energy Monitoring and Control. http://www.theowl.com/. Accessed: 2015-10-01.

[49] The World Bank. Country and Lending Groups. http://data.worldbank.org/about/country-and-lending-groups#Low_income. Accessed: 2015-17-11.

[50] Maherin Houssain Tonny. Performance Analysis of BRAC Solar Energy Program. 2009.

[51] Unites Nations Sustainability Goals. Energy. http://www.un.org/sustainabledevelopment/energy/. Accessed: 2015-09-12.

[52] University of New South Wales, Australia. There's a sunny future ahead for rooftop solar power: here's why. https://newsroom.unsw.edu.au/news/science-tech/there%E2%80%99s-sunny-future-ahead-rooftop-solar-power-here%E2%80%99s-why. Accessed: 2015-08-19.

[53] Frank Vignola, Joseph Michalsky, and Thomas Stoffel. *Solar and Infrared Radiation Measurements*. Taylor & Francis Group, 2012. ISBN 978-1-4398-5190-6. URL http://dx.doi.org/10.1201/b12367.

[54] Adriaan Van Der Welle and Bob Van Der Zwaan. An Overview of Selected Studies on the Value of Lost Load (VOLL). pages 5–25, 2007.

[55] Harry Wirth and Karin Schneider. Recent Facts about Photovoltaics in Germany. 2015.

[56] D. K. Yadav, Sai Pranith Girimaji, and T.S. Bhatti. Optimal hybrid power system design for rural electrification. *2012 2nd International Conference on Power, Control and Embedded Systems*, pages 1–6, dec 2012. doi: 10.1109/ICPCES.2012.6508125. URL http://ieeexplore.ieee.org/lpdocs/epic03/wrapper.htm?arnumber=6508125.

[57] A. Zelenka, R. Perez, R. Seals, and D. Renné. Effective accuracy of satellite-derived hourly irradiances. *Theoretical and Applied Climatology*, 62:199–207, 1999. ISSN 0177798X. doi: 10.1007/s007040050084.